Received: 30 April 2023 | Revised: 14 July 2023 | Accepted: 4 August 2023

DOI: 10.1111/ejn.16127

REGISTERED REPORT

EJN European Journal of Neuroscience FENS WILEY

Effects of transcranial magnetic stimulation (TMS) current direction and pulse waveform on cortico-cortical connectivity: A registered report TMS-EEG study

Giacomo Guidali[1] | **Agnese Zazio**[1] | **Delia Lucarelli**[1] | **Eleonora Marcantoni**[1] | **Antonietta Stango**[1] | **Guido Barchiesi**[2] | **Marta Bortoletto**[1]

[1]Neurophysiology Lab, IRCCS Istituto Centro San Giovanni di Dio Fatebenefratelli, Brescia, Italy

[2]Department of Philosophy, University of Milano, Milan, Italy

Correspondence
Marta Bortoletto, Neurophysiology Lab, IRCCS Istituto Centro San Giovanni di Dio Fatebenefratelli, via Pilastroni 4, 25125 Brescia, Italy.
Email: mbortoletto@fatebenefratelli.eu

Giacomo Guidali, Department of Psychology, University of Milano-Bicocca, Piazza dell'Ateneo Nuovo 1, Milan, Italy.
Email: giacomo.guidali@unimib.it

Present address
Giacomo Guidali, Department of Psychology, University of Milano-Bicocca, Milan, Italy.

Funding information
Italian Ministry of Health - funding Ricerca Corrente

Edited by: EJN Registered Reports Editors

Abstract

Transcranial magnetic stimulation (TMS)-evoked potentials (TEPs) are a promising proxy for measuring effective connectivity, that is, the directed transmission of physiological signals along cortico-cortical tracts, and for developing connectivity-based biomarkers. A crucial point is how stimulation parameters may affect TEPs, as they may contribute to the general variability of findings across studies. Here, we manipulated two TMS parameters (i.e. current direction and pulse waveform) while measuring (*a*) an early TEP component reflecting contralateral inhibition of motor areas, namely, M1-P15, as an operative model of interhemispheric cortico-cortical connectivity, and (*b*) motor-evoked potentials (MEP) for the corticospinal pathway. Our results showed that these two TMS parameters are crucial to evoke the M1-P15, influencing its amplitude, latency, and replicability. Specifically, (*a*) M1-P15 amplitude was strongly affected by current direction in monophasic stimulation; (*b*) M1-P15 latency was significantly modulated by current direction for monophasic and biphasic pulses. The replicability of M1-P15 was substantial for the same stimulation condition. At the same time, it was poor when stimulation parameters were changed, suggesting that these factors must be controlled to obtain stable single-subject measures. Finally, MEP latency was modulated by current direction, whereas non-statistically significant changes were evident for amplitude. Overall, our study highlights the importance of TMS parameters for early TEP responses recording and suggests controlling their impact in developing connectivity biomarkers from TEPs. Moreover,

Abbreviations: ANCOVA, analysis of covariance; AP, anterior–posterior; CCC, concordance correlation coefficient; EEG, electroencephalography; EMG, electromyography; ICA, independent component analysis; ICC, intraclass correlation coefficient; LM, latero-medial; M1, primary motor cortex; MEPs, motor-evoked potentials; MSO, maximum stimulator output; PA, posterior–anterior; rMT, resting motor threshold; rmANOVA, repeated measures analysis of variance; SD, standard deviation; SE, standard error; SOUND, source-estimate-utilizing noise-discarding algorithm; SSP-SIR, signal-space projection and source-informed reconstruction algorithm; TEPs, TMS-evoked potentials; TMS, transcranial magnetic stimulation.

these results point out that the excitability of the corticospinal tract, which is commonly used as a reference to set TMS intensity, may not correspond to the excitability of cortico-cortical pathways.

KEYWORDS
cortico-cortical connectivity, corticospinal connectivity, electroencephalography, motor cortex, TMS-EEG, TMS-evoked potentials, transcranial magnetic stimulation

1 | INTRODUCTION

Transcranial magnetic stimulation (TMS) in combination with electromyography (TMS-EMG) and electroencephalography (TMS-EEG) allows for the measurement of the transmission of physiological signals along corticospinal [i.e. motor-evoked potentials (MEPs)] and cortico-cortical tracts [i.e. TMS-evoked potentials (TEPs)], respectively.

TMS-EMG and TMS-EEG are widely employed in both basic and clinical research. MEPs provide established measures of corticospinal tract excitability and integrity, as well as intracortical facilitation/inhibition. They can highlight the involvement of the motor system in motor and cognitive performance and aid in the diagnosis of neurological disorders, for example, motor neuron disorders and multiple sclerosis (Bestmann & Krakauer, 2015; Di Lazzaro et al., 1999). TMS-EEG coregistration is becoming more important to understand brain dynamics and effective connectivity (Bortoletto et al., 2015). Specifically, TEPs are being evaluated as possible neurophysiological biomarkers for pathological conditions associated with alterations of cortico-cortical connectivity, such as psychiatric disorders like major depressive disorder and schizophrenia (Hui et al., 2019). TEPs can provide global measures of connectivity, that is, an integrated index of the overall response of cortical networks within the first hundreds of ms after the TMS pulse (e.g. Comolatti et al., 2019; Momi et al., 2021), and more specific indices of effective connectivity restricted to specific white matter tracts (e.g. Bortoletto et al., 2021; Koch, 2020).

A crucial point to be addressed for the development of connectivity biomarkers from MEPs and TEPs is how they are affected by changes in stimulation parameters such as pulse waveform, the direction of the induced current, and pulse duration. If different stimulation parameters (or different stimulators) across studies may impact latency, amplitude, and polarity of responses, they may contribute to the general variability in MEP (e.g. Corp et al., 2021; Davila-Pérez et al., 2018) and TEP findings (e.g. Bonato et al., 2006; Casula et al., 2018). In the last 30 years, the effects of stimulation parameters have been mainly studied on the corticospinal tract due to the relatively easy assessment of MEPs (e.g., Di Lazzaro et al., 2018; Di Lazzaro & Ziemann, 2013). Less is known about the impact of TMS parameters on responses generated in cortico-cortical pathways within the brain (i.e. TEPs).

Invasive measures of the corticospinal tract suggest that TMS pulse waveform and direction modulate the activation induced in the targeted neural population (Di Lazzaro et al., 2001). When the coil induces currents perpendicular to the central sulcus and the current direction flows in a posterior–anterior (PA) direction (i.e. the 'standard' 45° coil orientation for M1 stimulation), TMS pulses at the individual's resting motor threshold (rMT) intensity evoke I-waves in the corticospinal tract (Di Lazzaro et al., 2012). These waves are generated in superficial layers (i.e. II and III) of M1 by cortical interneurons, which transinaptically activate neurons of the pyramidal tract. When the current flows anterior–posterior (AP; i.e. in the reversed direction), the stimulation still evokes I-waves but with a longer latency and a smaller amplitude (Di Lazzaro et al., 1998, 2001, 2012). These results may suggest that these two current directions activate different neuronal populations in the superficial layers of M1 (Hamada et al., 2014; Spampinato, 2020). In contrast, when the coil induces currents flowing in a latero-medial (LM) direction, both a D-wave and I-waves are evoked. The D-wave has a shorter latency (approximately 1–2 ms) and higher amplitude than I-waves, and it is thought to originate by directly stimulating pyramidal tract neurons in layer V of M1 (Di Lazzaro et al., 1998, 2012; Di Lazzaro et al., 2018). Regarding the TMS pulse waveform, monophasic pulses have an initial high-rise phase responsible for neural stimulation, followed by a slow and smaller return current in the opposite direction (Di Lazzaro et al., 2018). Conversely, biphasic pulses include two waveforms, a forward and a reversed phase, with the former being slightly shorter and smaller than the latter (e.g. Corthout et al., 2001; Groppa, Oliviero, et al., 2012; Kammer, Beck, Erb, & Grodd, 2001; Maccabee et al., 1998; Weyh et al., 2005). Importantly, each phase induces a physiologically significant tissue current and evokes a more

complex sequence of neuronal activation (e.g. Barre et al., 2001; Maccabee et al., 1998; Sommer et al., 2006). However, the patterns of current direction modulation are still under investigation. For clarity, in the present work, we referred to the direction of induced current using a biphasic waveform as the direction of the second stimulation phase; for example, the current direction 'AP-PA' for biphasic pulses will be referred to as 'PA'.

If the corticospinal tract response is recorded noninvasively from the target muscle—for example, using superficial electrodes—current direction and pulse waveform modulate several measures, including resting motor threshold (rMT), MEP latency, and MEP amplitude (Di Lazzaro et al., 2018). In detail, rMT, defined as the minimal TMS intensity that produces an EMG response of at least 50 μV at rest in approximately half of the stimuli (Rossi et al., 2009), is higher for monophasic waveforms than biphasic ones and for the AP current direction than the PA one exploiting monophasic waveforms (Corp et al., 2021; Davila-Pérez et al., 2018; Kammer, Beck, Thielscher, et al., 2001; Sommer et al., 2006, 2018). Considering MEP latency, there is evidence that PA- and LM-evoked MEPs have shorter latency (approximately 1–3 ms) than AP-evoked ones, suggesting that these coil orientations activate different neuronal populations within M1 (Davila-Pérez et al., 2018; Di Lazzaro et al., 2001; D'Ostilio et al., 2016; Sommer et al., 2006; Terao et al., 1997; Werhahn et al., 1994). This difference in latency seems easier to detect for monophasic pulses than biphasic ones, likely due to the 'single' direction of stimulation of the former pulses (Sommer et al., 2006). Considering MEP amplitude, the data are more controversial: overall, it seems that biphasic waveforms elicit MEPs with a greater amplitude than monophasic waveforms (Corp et al., 2021), with no significant differences between coil orientations (Davila-Pérez et al., 2018; Sommer et al., 2018). However, the test–retest reliability of MEP amplitude seems lower than that of rMT and MEP latency; namely, rMT and MEP latency seem to be more stable within a single participant than MEP amplitude (Davila-Pérez et al., 2018).

Finally, considering TMS-EEG, to the best of our knowledge, only a few studies have investigated the contribution of current direction and pulse waveform (Bonato et al., 2006; Casarotto et al., 2010; Casula et al., 2018; Tervo et al., 2022). Specifically, Bonato et al. (2006), stimulating M1 with biphasic pulses, observed that PA and LM current direction evoked early TEPs (i.e. P30 and N45 components) with different polarity; however, a physiological interpretation of such a difference was not provided (Bonato et al., 2006). Casarotto et al. (2010) showed that by using different coil orientations over different brain areas, TEP morphology could vary considerably (Casarotto et al., 2010). Casula et al. (2018) reported a similar finding to Bonato et al. (2006), namely, a modulation of the polarity of early responses dependent on current direction following M1 stimulation. The authors found that the global mean field power, an index of TMS-evoked global cortical response, was higher after monophasic pulses than biphasic ones; nevertheless, no data were reported on the effects of current direction on specific TEP components and their latency (Casula et al., 2018). Recently, Tervo et al. (2022) showed how it is possible to optimize TMS effects by adjusting the orientation of the coil based on online trial-by-trial EEG response feedback, suggesting that coil orientation plays a crucial role in TEP recording (Tervo et al., 2022). Despite all this evidence, however, it remains unclear how pulse shape and current direction may modulate effective connectivity measures.

In the present study, we will extend previous findings by investigating responses generated in cortico-cortical pathways. Specifically, we focused our investigation on an early TEP component recently described by our research group, the M1-P15. M1-P15 is a positive peak over contralateral fronto-central electrodes arising approximately 15 ms after the TMS pulse over M1 and it reflects cortico-cortical inhibition in motor areas through the corpus callosum (Bortoletto et al., 2021). Indeed, its latency is predicted by a functional measure of transcallosal connectivity assessed with diffusion tensor imaging, such that the greater the mean diffusivity of the body of the corpus callosum, the shorter the M1-P15 latency. Furthermore, the amplitude of M1-P15 is positively related to the magnitude of a peripheral measure of interhemispheric inhibition, namely, the ipsilateral silent period (iSP) (Bortoletto et al., 2021).

In detail, we investigated the latency and amplitude of M1-P15 across different stimulation conditions by varying TMS coil orientation (to induce PA, AP, and LM current directions) and pulse waveform (monophasic or biphasic). Research in animal models shows that transcallosal signal transmission (Harris & Shepherd, 2015), similar to other cortico-cortical connections in the motor system, relies mainly on intratelencephalic neurons of M1 superficial (i.e. II and III) layers (McColgan et al., 2020; Sahni et al., 2020). These neurons should constantly be activated at an individual's rMT intensity (Di Lazzaro et al., 2012). Hence, PA, AP, and LM current directions—and monophasic/biphasic pulse waveforms—should all activate intratelencephalic M1 neurons, allowing us to observe M1-P15 independently of the stimulation parameters.

First, we investigated whether these TMS parameters affect M1-P15 latency, which has been proposed as a

measure of transcallosal conduction delay, and M1-P15 amplitude, which has been proposed as a measure of transcallosal motor inhibition (Bortoletto et al., 2021). In line with the effects on MEP latency (e.g. Davila-Pérez et al., 2018; D'Ostilio et al., 2016; Sakai et al., 1997; Sommer et al., 2006), we expected that the M1-P15 latency would be modulated according to the current direction, likely with higher latencies in the AP direction. Regarding the M1-P15 amplitude, the contrasting results on MEP amplitude (e.g., Corp et al., 2021; Davila-Pérez et al., 2018; Sommer et al., 2018) did not allow us to state clear hypotheses.

Second, we tested whether M1-P15 latency and amplitude show high replicability, including measures of agreement and reliability (de Vet et al., 2006). Agreement was estimated by the concordance correlation coefficient (CCC), which indicates how close two measurements are taken in the same condition or different conditions (Lin, 1989). Reliability was estimated using the intraclass correlation coefficient (ICC), which assesses how well a variable can distinguish between individuals by involving agreement among repeated measurements and the spread of subjects at once (McGraw & Wong, 1996). We assessed CCCs and ICCs by comparing M1-P15 latency and amplitude recorded in our six experimental blocks with those recorded in a (seventh) block where the same experimental parameters exploited in Bortoletto et al. (2021) were used. Considering that previous studies have shown high reliability of MEP latency and low reliability of MEP amplitude, we expected a similar pattern of results for M1-P15 (Davila-Pérez et al., 2018).

Third, we assessed the rMT in every experimental block as the *positive control* variable, namely, as the benchmark that our stimulation protocol had worked as expected from previous literature. Based on previous studies with monophasic waveforms, we hypothesized that PA and LM current directions led to lower rMT than AP (e.g. Corp et al., 2021; Davila-Pérez et al., 2018). Finally, we have also assessed MEP amplitude and latency in every block, seeking to shed light on the controversial results found in the literature.

Before running our study, we conducted a pilot experiment (see Supplementary Materials – Pilot experiment) to qualitatively assess whether the M1-P15 can also be recorded when both participants' hands are relaxed, as planned to be done during the experimental blocks of the present work. In fact, in the original work of Bortoletto et al. (2021), the ipsilateral (to stimulation) hand was kept slightly contracted during TMS-EEG. Hence, our pilot experiment aimed to test the feasibility of such an experimental modification.

2 | MATERIALS AND METHODS

2.1 | Participants

All recruited participants were right-handed, as assessed with the Edinburgh Handedness Questionnaire (Oldfield, 1971), with no contraindication to TMS (Rossi et al., 2009), and in the age range of 18 and 50 years. The study was conducted at the Neurophysiology Laboratory of the IRCCS Istituto Centro San Giovanni di Dio Fatebenefratelli (Brescia, Italy). It was performed in accordance with the ethical standard of the Declaration of Helsinki and has received approval from the local ethics committee (IRCCS Istituto Centro San Giovanni di Dio Fatebenefratelli, reference number: 102-2021).

2.2 | Sample size estimation and exclusion criteria

The study's sample size was estimated separately for the hypotheses (*a*) on M1-P15 modulations, (*b*) on the reliability of M1-P15 across conditions, and (*c*) on the *positive control* variable.

1. Regarding the hypotheses on M1-P15 modulations, considering that they derive from MEP studies and that the current literature does not provide evidence about M1-P15 in this direction, we considered the literature on the modulation of MEP latency. In a within-subject experiment by Sommer et al. (2006) with a similar experimental design (i.e. six different experimental conditions modulating pulse waveform and current direction), a significant difference was found between monophasic-evoked MEP latency recorded using PA (mean ± SD: 23.9 ± 2.12 ms) versus AP current direction (25.8 ± 2.08 ms; $p < .01$, $d = .9$). To account for the higher number of within-subject comparisons and the differences in the experimental design, as well as for possible publication bias (Anderson et al., 2017), we considered a smaller effect size of $d = .6$. Using the software G*Power 3.1 (Faul et al., 2009), with an alpha of .05 and a power of .9, the estimated sample size was 26 subjects.
2. For the investigation of M1-P15 replicability, we based the sample size estimation on the original study of Bortoletto et al. (2021), in which M1-P15 were recorded in two different experimental conditions. Specifically, in this study, the two conditions differed for the activity of the hand contralateral to TMS, which could be involved in a thumb-to-finger opposition movement task or at rest. We considered the correlation between M1-P15 recorded in the two

conditions as a measure of effect size for the latency and the amplitude separately. A correlation of $r = .87$ (for M1-P15 latency) and $r = .82$ (for M1-P15 amplitude) was found. Using the same parameters adopted for the previous estimations and a smaller effect size of $r = 0.6$, the sample size required was 27 participants.

3. Finally, the *positive control* of the present study was the replication of rMT modulation depending on the current direction and pulse waveform. Therefore, we also estimated the sample size for this variable. We based our calculation on a study by Davila-Pérez et al. (2018), in which a significant effect of ANOVA was found between participants' rMTs recorded using different current directions and pulse waveforms ($AP_{monophasic} = 75 \pm 7.1\%$; $PA_{monophasic} = 66.2 \pm 4.5\%$; $PA_{biphasic} = 59.7 \pm 9.1\%$; $F_{2,20} = 9.28$, $p = .001$; *eta-squared* $= .96$). Adopting the same parameters exploited in the previous estimations and a smaller effect size of *eta-squared* $= 0.6$, the sample size is 28 participants.

Taking together all these sample size estimations, to counterbalance the order of the experimental conditions and to take into account possible dropouts or outliers, we planned to recruit 35 participants. According to the sample size estimation, if the final analysed sample was lower than 28 participants, we would have recruited more participants to reach this number of analysed subjects.

In detail, exclusion criteria for a participant were (*a*) to not complete all the experimental blocks due to personal or technical issues (e.g. discomfort during TMS, hardware/software failures); (*b*) TMS intensity (i.e. 110% of rMT) in at least one experimental condition exceeding 90% of maximal stimulator output; (*c*) target variables (i.e. M1-P15 and/or MEP amplitude and latency) exceeding ±2.5 SD from the mean of the group (in the worst-case scenario, we expect to exclude no more than three participants using this criterion); and (*d*) more than 30% of the trials within each experimental block marked as artefactual during EEG preprocessing (see Section 2.6).

2.3 | Experimental procedure

The experiment consisted of a single session in a within-subject design lasting approximately 3 h and 30 min. Each participant underwent seven blocks of TMS-EEG coregistration in counterbalanced order according to a Latin square design. Participants sat in a dimly lit room facing a fixation cross on a computer screen, with their forearms resting on a table. The EEG cap and EMG electrodes were mounted in the preparation phase, and neuronavigation procedures were carried out using SofTaxic Optic 3.4 neuronavigation software (EMS, Bologna, Italy; www.softaxic.com) to allow monitoring of the position of the TMS coil throughout the experiment. On the neuronavigation software, we had set the threshold to 3 mm to minimize the variability across pulses and experimental blocks. SofTaxic software does not allow us to record the position of the coil for each pulse, so we do not have offline control of the trial-by-trial variability in coil positioning. However, the experimenter constantly monitored that the coil was within the defined threshold.

Then, the optimal motor hotspot for the right *abductor pollicis brevis* (APB) muscle was found using the biphasic stimulator and the PA current direction (as in Bortoletto et al., 2021). The location of participants' motor 'hotspot' was assessed by recording MEPs from APB. The APB motor hotspot over the left hemisphere was then used as the stimulation target throughout the experiment, regardless of the exploited TMS pulse waveform and current direction. After the determination of the motor hotspot, EEG electrodes were filled with electroconductive gel, and skin-electrode impedance was checked.

Finally, seven blocks of stimulation were carried out, each including consecutive assessment of the rMT, TMS-EMG, and TMS-EEG recording (Figure 1).[1] The rMT assessed at the beginning of each block was employed in the following TMS-EMG and TMS-EEG recordings. TMS was set according to the exploited TMS pulse waveform (monophasic, biphasic) and the induced current direction (PA, AP, LM). Participants were instructed to keep their right hand relaxed and fix a white cross appearing in the centre of a PC screen at a distance of 70 cm from their eyes. Each block lasted approximately 15 min.

We have also introduced a condition where M1-P15 was recorded using the same parameters as Bortoletto et al.'s (2021) original research. In this block, participants were stimulated using biphasic PA pulses, and at the same time, their left hand was slightly contracted (rather than relaxed, as in the other six blocks). During TMS-EEG, participants were instructed to keep their left

[1]In the Stage 1 *in principle acceptance* version of the manuscript, MEPs were planned to be recorded from EMG during TMS-EEG blocks. However, after the first few recordings, we noticed a decay artefact in the EMG that could affect the measurement of MEP latency and that could possibly be due to a single ground shared for EMG and EEG. To avoid this problem, we separated the recording of MEPs from that of TMS-EEG by adding recording blocks specifically dedicated to MEPs in which the ground electrode was positioned over the forearm. This change in protocol received editorial approval on 28 July 2022. All the 40 participants of the study underwent this modified version of the original protocol, and, at the time of approval, data had been collected from 18 participants over 40, but they had not been preprocessed yet.

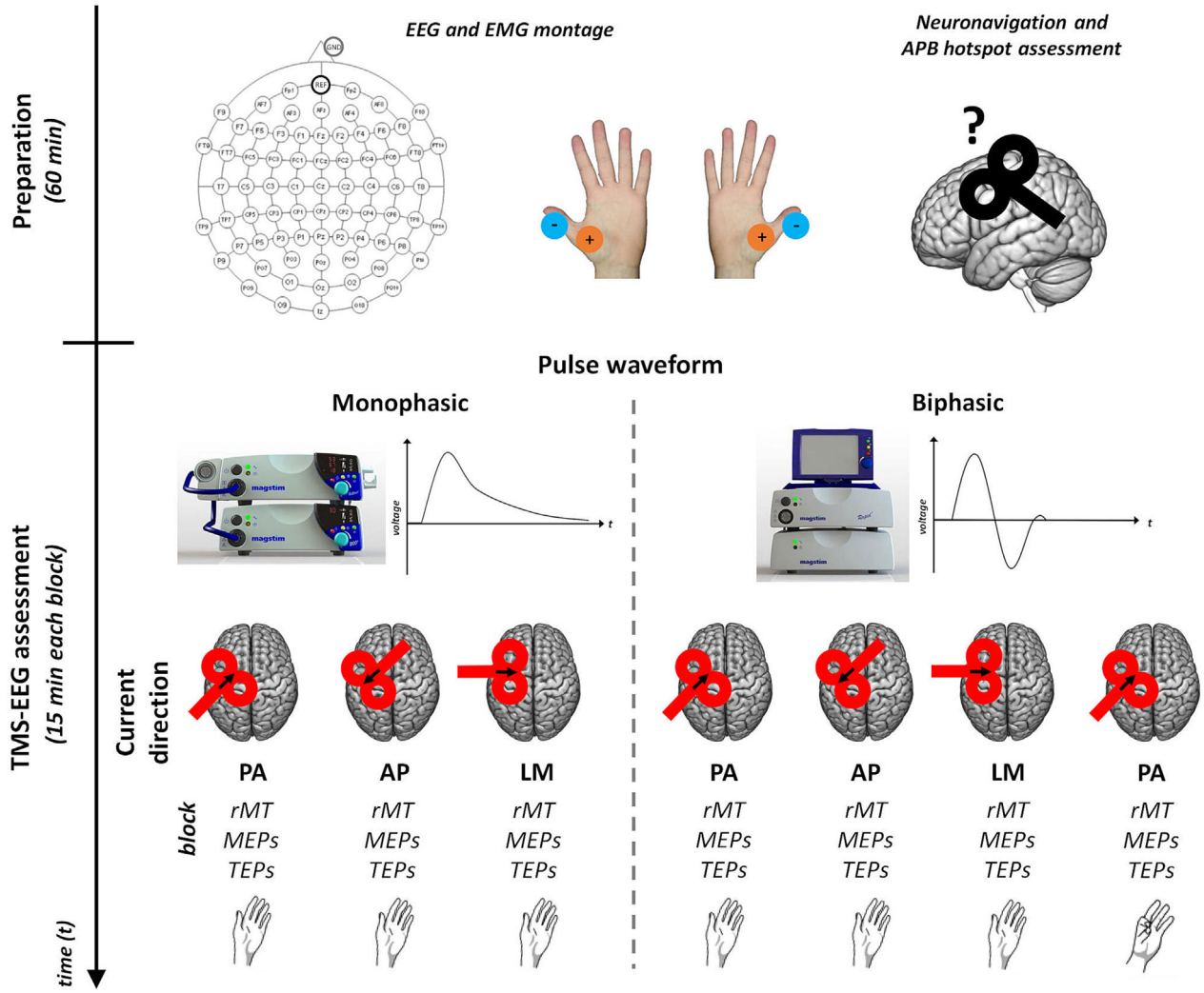

FIGURE 1 Experimental procedure. Black arrows depicted over the stylized TMS coils indicate the direction of the current induced in M1. Biphasic waveforms indicate the current direction of the second stimulation phase (see main text for further information). In the experimental block replicating the stimulation parameters of Bortoletto et al. (2021) (i.e. the seventh block from the left in the figure), the left hand—ipsilateral to TMS—was kept slightly contracted rather than at rest. The order of the seven blocks was counterbalanced across participants.

(ipsilateral to TMS) hand slightly contracted (i.e. between 20% and 40% of their maximal contraction force—preliminarily assessed by pressing as strong as possible the left-hand thumb on a pressure sensor put on the index finger). Throughout the block, the correct level of contraction of the left-hand APB was monitored online through visual cues appearing on the PC screen, indicating to the participant whether the contraction level fell out of the target range. TMS pulses were not delivered until the contraction level fitted within the target range.

As mentioned above, in six out of seven experimental blocks, the participant's right and left hands were kept at rest. This differs from Bortoletto et al.'s (2021) original study, in which the right (ipsilateral to stimulation) hand was slightly contracted. Hence, we have preliminarily run a pilot experiment with the aim of verifying that M1-P15 can be obtained both with the ipsilateral hand contracted or relaxed (see Supplementary Materials – Pilot experiment).

2.4 | TMS

According to the experimental block, TMS was delivered using a figure-of-eight coil (Magstim model Alpha B.I. Coil Range, diameter: 70 mm) connected to one of two different commercial stimulators. In monophasic blocks, we have used a Magstim 200^2 stimulator; in biphasic blocks, we have used a Magstim Rapid^2 stimulator (Magstim, Whitland, UK).

The pulse waveform and the current direction changed for each block of stimulation. For PA blocks, the coil was held tangentially to the scalp with its wings at 45° with respect to the midline. For AP blocks, the coil was

tilted 180° from the PA position. For LM blocks, the coil was held with its wings at 90° with respect to the midline (see Figure 1). During EMG recording, 20 TMS pulses were delivered for each block with an interstimulus interval jittered between 4000 and 6000 ms using an ad hoc created MATLAB script, which can be found at: https://gin.g-node.org/Giacomo_Guidali/Guidali_et_al_2023_EJN_RR/src/master/Script%20task (MATLAB R2020b, The MathWorks, Natick, MA, USA). During TMS-EEG, 80 pulses were delivered with the same parameters adopted for MEP recording. The intensity was set equal to 110% of the rMT, as measured at the beginning of each block by employing the best parameter estimation by sequential testing (PEST) procedure (i.e. maximum-likelihood threshold-hunting procedure) (Awiszus, 2003; Dissanayaka et al., 2018).

At the beginning of the experiment, a thin layer of foam was placed under the TMS coil to reduce sensory stimulation associated with TMS, and white noise was played through noise-cancelling earphones (Biabani et al., 2019). The volume of the white noise was individually adjusted to mask the TMS click but avoid hearing discomfort, as done in previous studies by our group (Bortoletto et al., 2021; Zazio et al., 2022). Throughout the experiment, the TMS coil was held by a trained experimenter and adjusted according to the information provided by the neuronavigation system.

2.5 | EEG and EMG recording

A TMS-compatible EEG system (g.HIamp multichannel amplifier, g.tec medical engineering GmbH) was employed to record EEG and electromyography (EMG). EEG was measured from 74 electrodes (EasyCap, Brain Products GmbH, Munich, Germany) placed on the scalp according to the 10–10 international system and referenced to FPz. The ground was placed on the tip of the nose. EMG was collected from both the right- and the left-hand APB muscles with bipolar belly tendon montage, that is, one electrode (Ag/AgCl pre-gelled surface electrodes, Friendship Medical, Xi'an, China) placed over the muscle belly and one electrode, set as the reference, placed over the metacarpophalangeal joint of the thumb (Figure 1). During MEP recording, the ground was placed on the forearm. The sampling rate was set to 9.6 kHz, and the skin-electrode impedance was kept below 5 kΩ. During EEG and EMG recording, high-pass filters (i.e. 1 Hz—order: 1 and 10 Hz—order: 3, respectively) were applied online for visualization purposes. Before data acquisition, a visual inspection was made to guarantee that background noise from the APB channels was smaller than 20 μV. Moreover, EEG and EMG signals were visually inspected before and during the recordings to avoid obvious artefacts, for example, long decays, noisy channels, and line noise.

2.6 | EEG preprocessing

TEP preprocessing followed a pipeline that is currently used for TMS-EEG data in our lab, adapted from our previous studies targeting M1-P15 (Bortoletto et al., 2021; Zazio et al., 2022). The pipeline has been implemented in MATLAB R2020b (The MathWorks, Natick, MA, USA) with custom scripts combining EEGLAB v.2020.0 (Delorme & Makeig, 2004) and FieldTrip v.20190905 functions (Oostenveld et al., 2011) and two analysis methods, namely, the source-estimate-utilizing noise-discarding (SOUND) algorithm (Mutanen et al., 2018) and the signal-space projection and source-informed reconstruction (SSP-SIR) algorithm (Mutanen et al., 2016). The pipeline can be found at: https://gin.g-node.org/Giacomo_Guidali/Guidali_et_al_2023_EJN_RR/src/master/Script%20preprocessing%20EMG-EEG/preprocessingTEP_pipeline.m. If not otherwise specified, default parameters for EEGLAB and FieldTrip functions were used.

For every participant, each experimental condition was preprocessed separately. The steps of the pipeline are reported below according to order. Continuous EEG was interpolated around the TMS pulse (between −1 and 2 ms) high-pass filtered (1 Hz windowed sinc FIR filter, order 31680, using default parameters of EEGLAB function 'pop_eegfiltnew'), downsampled to 4800 Hz and epoched around TMS pulse (from −700 to 700 ms). Measurement noise was reduced with SOUND, using a spherical-head-3-layer model-based for the lead-field matrix and the regularization parameter $\lambda = .1$, as in the original paper of Mutanen et al. (2018). Then, the following steps were performed: (a) a first automatic artefact rejection using the EEGLAB function 'pop_jointprob'—which rejects artefacts in an EEG dataset using joint probability of the recorded electrode or component activities observed at each time point. This function, as input, requires specifying a threshold in terms of standard deviations (SD) that the signal within an epoch needs to exceed to be discarded; we will set this value at 5 SD and (b) an independent component analysis (ICA) selectively for ocular artefact correction using the EEGLAB function 'pop_runica' (infomax algorithm, 73 channels included, 72 ICA components computed). ICA components were visually inspected and rejected according to topographic and spectral patterns typical of vertical and horizontal ocular movements. Subsequently, TMS-evoked muscular artefacts in the first 50 ms were removed using SSP-SIR with the same parameters adopted as in the original work by Mutanen et al. (2016). Then, epochs were low-pass filtered

at 70 Hz (IIR Butterworth filter, order 4, using the EEGLAB function 'pop_basicfilter') and re-referenced to the average of TP9-TP10. Finally, after a second artefact rejection (visual inspection of epochs as a final check for residual artefacts), TMS-EEG data were epoched between −200 and 400 ms, baseline corrected from −200 to −2 ms before the TMS pulse, transformed into FieldTrip structure and averaged over trials. M1-P15 was identified as a positive TEP component peaking over the right frontocentral electrodes (contralateral to stimulation) at approximately 15 ms in the grand average of each experimental block. After averaging the signal from the frontocentral electrodes corresponding to the peak location of M1-P15 (i.e. F4 and FC4), we measured its amplitude and latency in each experimental condition as the peak in the window between 7 and 25 ms. Finally, the presence of M1-P15 was visually assessed (for a similar procedure, see Bortoletto et al., 2021; Zazio et al., 2022).

2.7 | EMG preprocessing

MEPs from right-hand APB muscle were analysed using an ad hoc created MATLAB script (https://gin.g-node.org/Giacomo_Guidali/Guidali_et_al_2023_EJN_RR/src/master/Script%20preprocessing%20EMG-EEG/MEP_pipeline.m). Preliminary, artefactual decay after TMS was corrected by interpolating the trace around the TMS pulse. Then, EMG data were bandpass filtered between 10 and 2500 Hz by applying a notch filter at 50 Hz. Following visual inspection, trials with artefacts (muscular or background noise) deviating from 100 μV in the 50 ms before the TMS pulse were excluded from the analysis. Then, MEP peak-to-peak amplitudes were calculated in each trial in the time window between 15 and 50 ms from the TMS pulse. Trials with MEPs smaller than 50 μV were discarded. The MEP latency was computed as the time interval (in ms) between the TMS pulse and the onset of the MEP.

2.8 | Statistical analysis

M1-P15 latency and amplitude, as well as MEP latency and amplitude, were separately analysed through 2 × 3 within-subject repeated-measures analysis of variance (rm-ANOVA) with the factors 'Pulse waveform' (monophasic, biphasic) and 'Current direction' (PA, AP, LM). Significant main effects and interactions were further explored with post hoc tests by applying the Tukey correction for multiple comparisons. If data sphericity was not confirmed by Mauchly's test, the Greenhouse–Geisser correction was applied. *Partial eta-squared* (η_p^2—for rm-ANOVAs) and Cohen's *d* (for *t*-tests) have been reported as effect size values. Before running these analyses, to make the data distribution closer to normality, we have transformed the raw data with three commonly used transformations for continuous variables: (*a*) square root [i.e. $\sqrt{(raw\,data)}$]; (*b*) base-ten logarithm [i.e. $\log_{10}(raw\,data)$]; and (*c*) inverse transformation [i.e. $\frac{1}{raw\,data}$]. To account for possible negative values, as well as values between 0 and 1, when applying these transformations, we added a constant to the raw data values, thus anchoring the minimum of our distribution(s) to 1 (Osborne, 2010). Then, we selected among raw data and these three transformations the one showing the best fit to a normal distribution using Cullen–Frey graphs and the 'fitdistrplus' package in R (Delignette-Muller & Dutang, 2015; https://cran.r-project.org/web/packages/fitdistrplus/index.html). If none of these transformations makes the data distribution close enough to normality, that is, the transformed distribution presents values of an excess kurtosis between −2 and 2 and skewness between −1 and 1 (George & Mallery, 2019), a robust one-way rmANOVA based on trimmed means (20% trimming level) with six factors (i.e. $AP_{monophasic}$, $PA_{monophasic}$, $LM_{monophasic}$, $AP_{biphasic}$, $PA_{biphasic}$ and $LM_{biphasic}$) was conducted on the raw data (Mair & Wilcox, 2020). Otherwise, we have proceeded with the 2 × 3 rmANOVAs described before.

Replicability of M1-P15 latency and amplitude between different within-subject conditions were assessed using two different indices: (*a*) CCC and (*b*) ICC. In detail, we assessed CCCs and ICCs by comparing each M1-P15 latency and amplitude recorded in the six main experimental blocks with the ones recorded in the block replicating the parameters used in the original study by Bortoletto et al. (2021). CCCs and ICCs were calculated using the CCC (King et al., 2007; Lin, 1989) and the ICC formula (model: two-way mixed; type: single measurement; definition: absolute agreement) (Koo & Li, 2016; McGraw & Wong, 1996), respectively.

For our *positive control* condition, rMT data were analysed through planned comparisons using robust statistics (i.e. Yuen's trimmed mean *t*-test, one-tailed, 20% trimming level) (Mair & Wilcox, 2020; Yuen, 1974): In detail, according to our a priori hypothesis (see Section 1), we have tested that, using monophasic waveforms, PA and LM current directions lead to lower rMT than AP directions.

In all analyses, the statistical significance was set at $p < .05$. For each variable, the mean ± standard error (SE) was reported. Graphical representations followed the guidelines reported by Rousselet et al. (2016), and confidence intervals for the effects were reported. Statistical analyses were performed using Jamovi (Version 2.3.21; The Jamovi Project, 2022) and R Studio (Version 1.2.5019; R Core Team, 2019).

Stage 1 in principle acceptance (IPA) version of the manuscript can be found at Open Science Framework (OSF): https://osf.io/rqzfm.

3 | RESULTS

3.1 | Registered analysis

3.1.1 | Final sample

Forty participants [24 females, median age (minimum–maximum): 26 years (22–49 years); median education: 16 years (13–21 years)] were recruited for the present study. Considering predefined exclusion criteria, 12 participants were not included in the analyses for the following reasons: (a) Two participants did not complete the experiment due to technical issues during EEG recording; (b) six participants were excluded due to TMS intensity exceeding 90% of maximal stimulator output in at least one experimental condition; (c) four participants were excluded because target variables exceeded ±2.5 SD from the mean of the group. Hence, the final analysed sample included 28 participants [15 females, median age: 26 years (22–49 years); median education: 16 years (13–21 years); median Edinburgh score: 83% (42%–100%)].

3.1.2 | M1-P15 extraction

TEP grand average and topographical maps of the M1-P15 found in each condition are depicted in Figure 2.

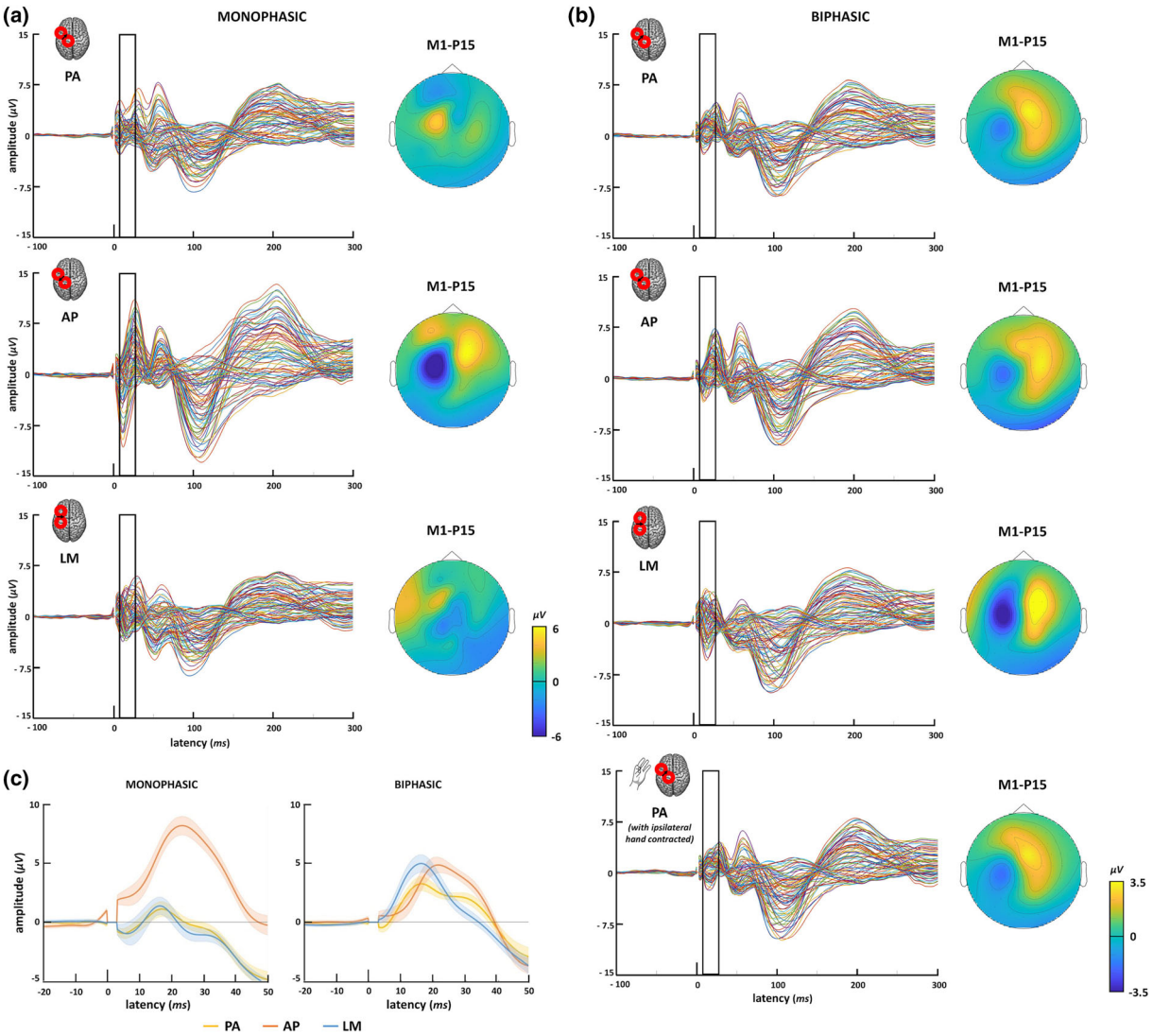

FIGURE 2 TEP grand average for monophasic and biphasic conditions. Grand average of TEPs and related topography of the M1-P15 between 7 and 25 ms in monophasic (a) and biphasic (b) conditions. (c) Grand average of M1-P15 (extracted by pooling F4 and FC4 electrodes) in the six main experimental conditions (SE represented by shaded error bars).

Values of M1-P15 amplitude and latency were extracted by pooling F4 and FC4 electrodes as in the study by Zazio et al. (2022), and individual values are plotted in Figure S1. For the number of ICA and SSP-SIR components removed in the preprocessing for every participant and in each condition, as well as the number of epochs rejected due to artefacts, see Tables S1–S3. Two researchers (GG and AZ) checked ICA and SSP-SIR components independently and compared them for the third and definitive selection.

3.1.3 | M1-P15 amplitude

M1-P15 amplitude was analysed with 2 × 3 rmANOVA with factors 'Pulse waveform' and 'Current direction', as there was not enough evidence that the distributions of the values were not normal. M1-P15 amplitude was significantly modulated by 'Current direction' ($F_{2,54} = 40.48$, $p < .001$, $\eta_p^2 = .6$) and by its interaction with 'Pulse waveform' ($F_{2,54} = 43.25$, $p < .001$, $\eta_p^2 = .616$). The main effect of 'Pulse waveform' did not reach statistical significance ($F_{1,27} = .53$, $p = .47$, $\eta_p^2 = .019$). In detail, monophasic AP current direction evoked the highest M1-P15 amplitude: its values (8.9 ± .7 μV) were higher than the ones recorded in monophasic PA and LM directions (PA = 1.2 ± .6 μV; $t_{27} = 9.5$, $p < .001$, $d = 1.79$; LM = 2.7 ± .7 μV; $t_{27} = 7.61$, $p < .001$, $d = 1.44$) and in all biphasic conditions (PA = 3.5 ± .4 μV; $t_{27} = 6.94$, $p < .001$, $d = 1.31$; AP = 4.8 ± .4 μV; $t_{27} = 6.18$, $p < .001$, $d = 1.17$; LM = 5.4 ± .6 μV; $t_{27} = 5.07$, $p < .001$, $d = .96$). Furthermore, monophasic PA and LM led to the lowest M1-P15 amplitude: PA evoked lower M1-P15 amplitude than the three biphasic conditions (PA: $t_{27} = -3.93$, $p = .006$, $d = -.74$; AP: $t_{27} = -5.49$, $p < .001$, $d = -1.04$; LM: $t_{27} = -5.92$, $p < .001$, $d = -1.12$) and LM current direction led to lower amplitude values than the same direction for biphasic stimulation ($t_{27} = -4.19$, $p = .003$, $d = -.79$). Finally, among biphasic stimulation conditions, LM led to higher M1-P15 amplitude than PA direction ($t_{27} = 3.5$, $p = .018$, $d = .66$) (Figure 3a).

3.1.4 | M1-P15 latency

Raw data of M1-P15 latency followed a non-normal distribution, and none of the planned transformations made the distribution closer to normality (Table S4). Hence, we proceeded with a robust one-way rmANOVA with six factors on raw data (Mair & Wilcox, 2020). Post hoc comparisons were performed using linear contrasts as described in Mair and Wilcox (2020). Results showed a statistically significant effect of TMS parameters on M1-P15 latency ($F_{3.71,\ 63.1} = 11.73$, $p < .001$). Post hoc comparisons revealed that AP current direction in both monophasic and biphasic waveforms led to slower M1-P15 latency values (monophasic: 20.5 ± 1 ms; biphasic: 21.5 ± .6 ms; these two conditions present no statistically significant values: $\Psi = -.02$, $p = .971$) than the ones recorded in PA and LM directions ($AP_{monophasic}$ vs. $PA_{monophasic} = 16.1 \pm .1$ ms; $\Psi = 4.25$, $p = .003$; vs. $LM_{monophasic} = 16.7 \pm .9$ ms; $\Psi = 5.41$, $p < .001$; vs. $PA_{biphasic} = 17 \pm .9$ ms; $\Psi = 5.17$, $p = .002$; vs. $LM_{biphasic} = 15.3 \pm .8$ ms; $\Psi = 4.46$, $p < .001$. $AP_{biphasic}$ vs. $PA_{monophasic}$: $\Psi = 3.16$, $p = .016$; vs. $LM_{monophasic}$: $\Psi = 4.71$, $p = .006$; vs. $PA_{biphasic}$: $\Psi = 4.82$, $p = .005$; vs. $LM_{biphasic}$: $\Psi = 3.96$, $p = .01$) (Figure 3b).

3.1.5 | Reliability and agreement of M1-P15

Considering ICC of M1-P15 latency and amplitude between the block with the contracted hand (Bortoletto et al., 2021) and the six main experimental blocks with resting hands, good reliability (i.e. ICC > .75; Koo & Li, 2016) was found only for M1-P15 amplitude in biphasic PA stimulation (ICC = .768), that is, between the condition in which participants contracted the hand ipsilateral to stimulation and the condition exploiting the same stimulator parameters with relaxed ipsilateral hand. All other comparisons—both on M1-P15 amplitude and latency—showed poor ICC values (all ICC values <.5; see Table 1).

The same pattern of results was found for the CCC (Figure 4), as the ICC and CCC had very similar values. It is indeed possible in some cases that they are equivalent, as it has been highlighted that the agreement measured with the CCC depends on the variability in the sample (Barnhart et al., 2007; Carrasco & Jover, 2003).

We also performed an explorative analysis on ICC and CCC by excluding the few cases which did not show a clear M1-P15 peak (see Section 3.2.4).

3.1.6 | MEP amplitude

MEP amplitude followed a non-normal distribution, and transforming these values by applying a base-ten logarithm transformation made the distribution closer to normality (Table S5); hence MEP amplitude was analysed on these transformed values with a 2 × 3 rmANOVA. The rmANOVA showed no statistically significant effect of the interaction 'Pulse waveform' × 'Current direction' ($F_{2,54} = 2.76$; $p = .072$; $\eta_p^2 = .093$) neither of the factors 'Pulse waveform' ($F_{1,27} = 1.39$; $p = .249$; $\eta_p^2 = .049$) and

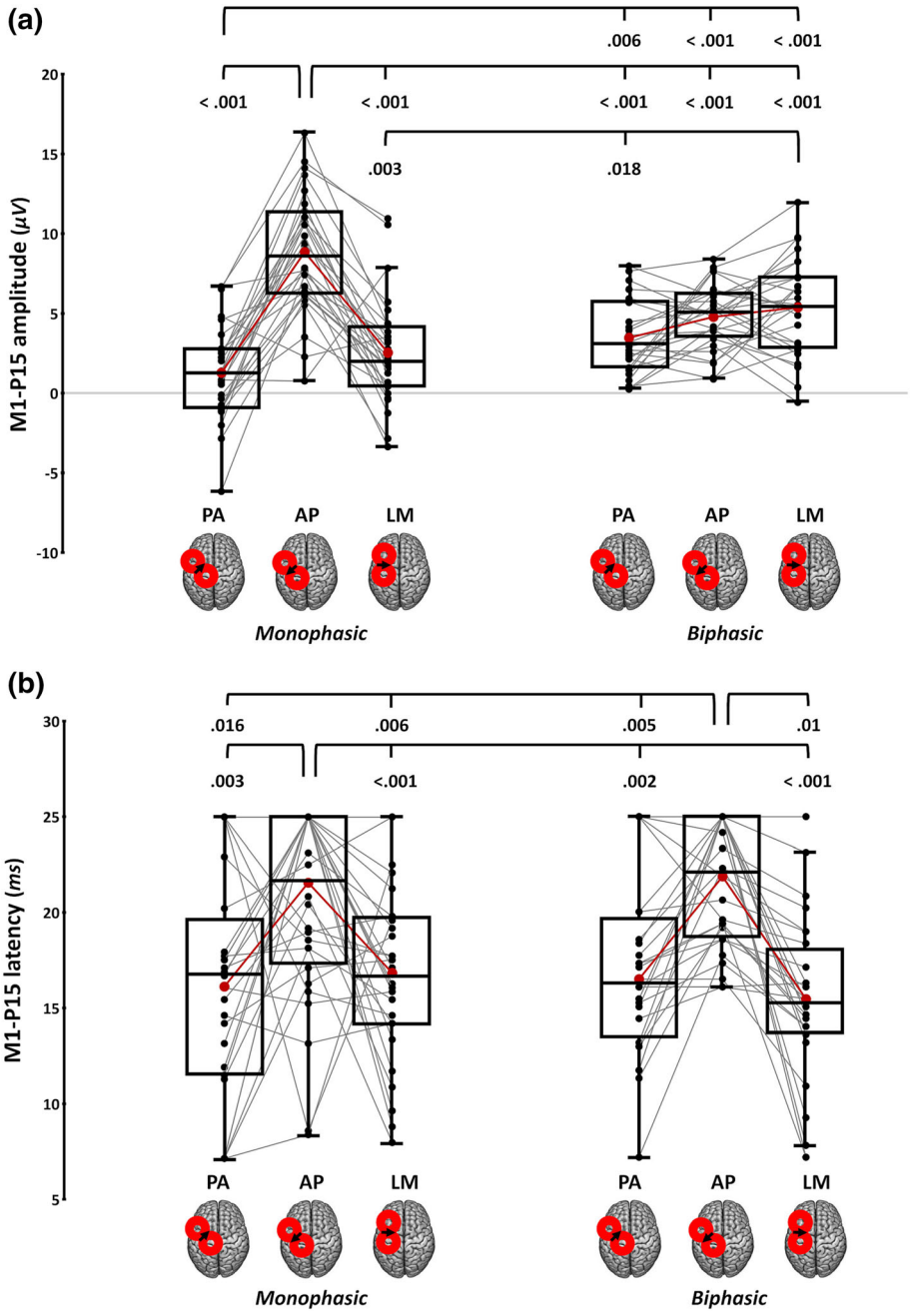

FIGURE 3 M1-P15 results. Amplitude (a) and latency (b) of the M1-P15 component in the six main experimental conditions. Black arrows depicted over the stylized TMS coils indicate the direction of the current induced in M1. In the box-and-whiskers plots, red dots and lines indicate the means of the distributions. For M1-P15 amplitude, they indicate 20% trimmed means. The centre line denotes their median values. Black dots and grey lines show individual participants' scores. The box contains the 25th to 75th percentiles of the dataset. Whiskers extend to the largest observation, which falls within the 1.5 times interquartile range from the first/third quartile; significant *p* values of corrected post hoc comparisons are reported.

'Current direction' ($F_{2,54} = 1.46$; $p = .242$; $\eta_p^2 = .051$). Therefore, $\log_{10}$ MEP amplitude was significantly modulated by neither the pulse waveform nor the current direction (Figure 5a).

3.1.7 | MEP latency

MEP latency was measured with a new automatized method recently developed by Bigoni et al. (2022) and by manually adjusting the computed onset in trials where its value was considered inaccurate (about 20% of trials on average) by two independent researchers (GG and DL). Data were analysed with a 2 × 3 rmANOVA on raw data as there was not enough evidence that the distributions of the values were not normal. MEP latency was significantly modulated by 'Current direction' ($F_{2,54} = 51.4$, $p < .001$, $\eta_p^2 = .656$) and by its interaction with 'Pulse waveform' ($F_{1.54,41.6} = 6.04$, $p = .009$, $\eta_p^2 = .183$). The main effect of the factor 'Pulse waveform' did not reach statistical significance ($F_{1,27} = 1.84$, $p = .186$, $\eta_p^2 = .064$). In detail, MEP latency was longer in the AP conditions, both for monophasic (25.4 ± .3 ms) and biphasic (24.9 ± .3 ms) stimulation, than the ones recorded using PA and LM directions, both for monophasic (PA = 24.2 ± .3 ms; LM = 24.2 ± .3 ms) and biphasic waveforms

TABLE 1 ICC and CCC values obtained by comparing each M1-P15 latency and amplitude recorded in the six main experimental blocks with the ones recorded in the block replicating the parameters used in the previous studies of our research group (Bortoletto et al., 2021; Zazio et al., 2022)—that is, ipsilateral (to TMS) hand contracted and biphasic PA current direction.

		Amplitude		Latency	
Biphasic PA with ipsilateral hand contracted versus		**ICC**	**CCC**	**ICC**	**CCC**
Biphasic	PA	**.768**	**.761**	.287	.28
	AP	.178	.174	.142	.137
	LM	.208	.202	.163	.158
Monophasic	PA	.219	.213	.341	.333
	AP	.014	.0134	.089	.086
	LM	.306	.298	−.061	−.059

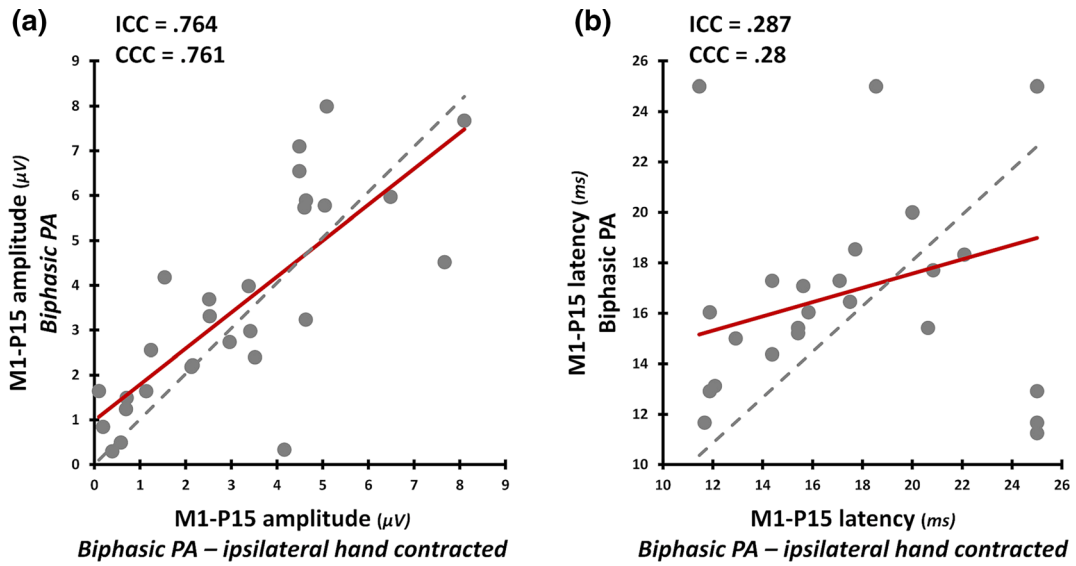

FIGURE 4 ICC and CCC results. Concordance plots between M1-P15 amplitude (a) and M1-P15 latency (b) in the two blocks where TMS is delivered by exploiting biphasic pulse waveform and PA current direction. Dotted grey line: expected regression line if the two measures were perfectly correlated. Straight red line: actual regression line. It has to be noted that our ICC estimation does not take measurement error into account.

(PA = 24.3 ± .3 ms; LM = 24.2 ± .3 ms; see Table 2 for post hoc comparisons). Furthermore, AP direction led to longer MEP latency in monophasic stimulation than in biphasic stimulation ($t_{27} = 3.22$, $p = .035$, $d = .61$) (Figure 5b).

3.1.8 | rMT for monophasic pulse waveform

Results of robust paired samples *t*-tests replicated findings already reported in literature on the effects of current direction in monophasic stimulation and supported the effectiveness of the experimental manipulation of current direction: Applying AP current direction led to higher rMT values [66 ± 1.9% maximum stimulator output (MSO)] than both PA (50.2 ± 1.5% MSO; $t_{17} = -10.87$, $p < .001$, $d = .811$) and LM directions (55.1 ± 1.8% MSO; $t_{17} = -6.07$, $p < .001$, $d = .636$). Furthermore, rMT found using PA direction was lower than the rMT found using LM ($t_{17} = -2.57$, $p = .02$, $d = .37$) (Figure 6).

For a comprehensive picture of the impact of the current direction on rMT, we have also analysed changes in rMT for different current directions in biphasic conditions; these exploratory analyses can be found in the Supplementary Materials – rMT in biphasic conditions.

3.2 | Exploratory analysis

Besides the planned statistical analysis mentioned above, we have conducted exploratory analyses to understand

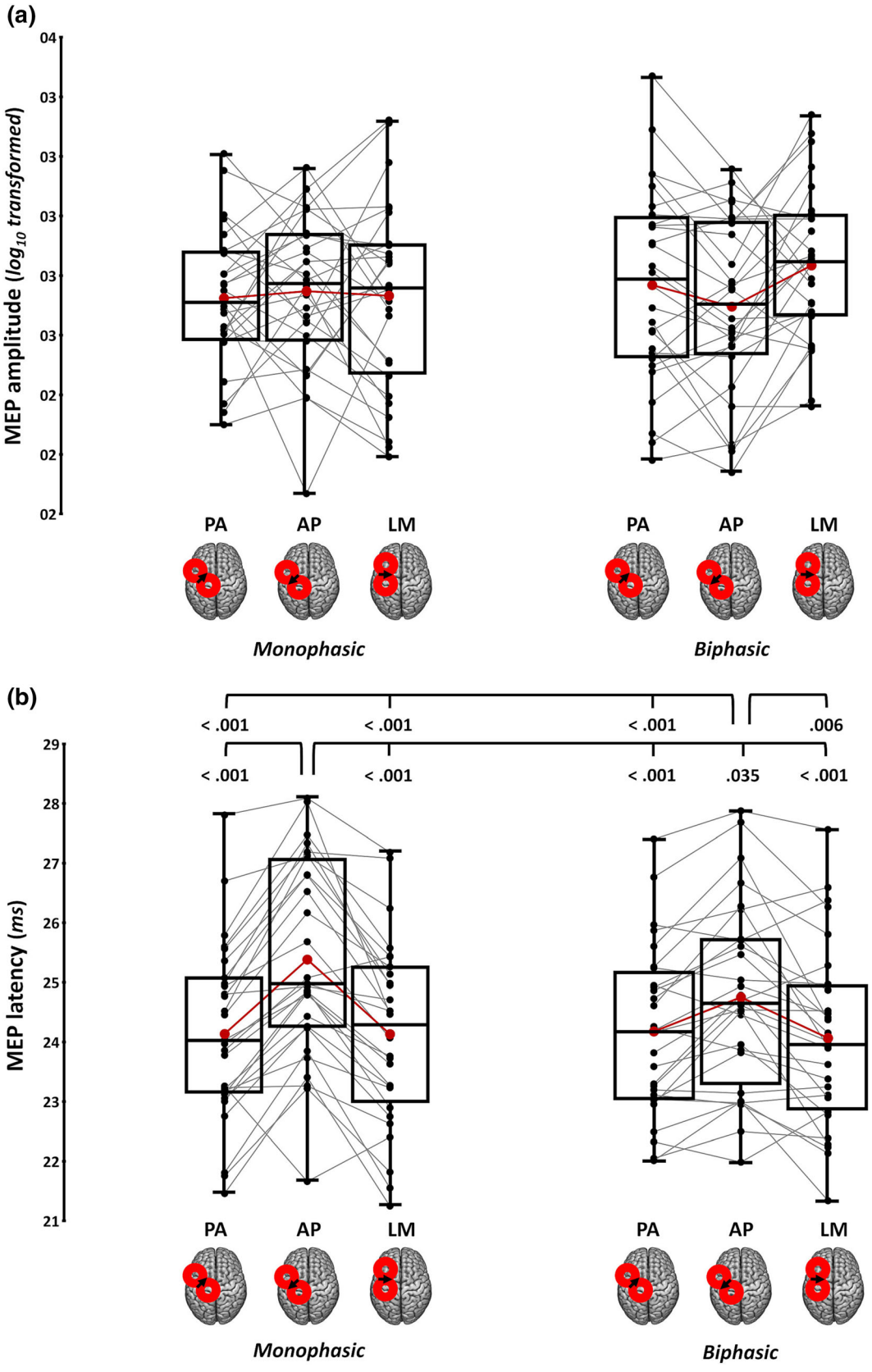

FIGURE 5 Legend on next page.

FIGURE 5 MEP results. Log_{10} amplitude (a) and latency (b) of MEPs in the six main experimental conditions. Black arrows depicted over the stylized TMS coils indicate the direction of the current induced in M1. In box-and-whiskers plots, red dots and lines indicate the means of the distribution, and the centre line denotes their median values. Black dots and grey lines show individual participants' scores. The box contains the 25th to 75th percentiles of the dataset. Whiskers extend to the largest observation, which falls within the 1.5 times interquartile range from the first/third quartile; significant *p* values of corrected post hoc comparisons are reported.

TABLE 2 Post hoc comparisons (Tukey corrected) for MEP latency values between the two conditions recorded with AP direction and the other experimental conditions.

	Pulse waveform	Current direction	t_{27}	*p* (Tukey corrected)	Cohen's *d*
AP monophasic versus	Monophasic	PA	7.51	<.001	1.42
		LM	7.24	<.001	1.37
	Biphasic	PA	7.05	<.001	1.33
		LM	7.04	<.001	1.33
AP biphasic versus	Monophasic	PA	4.96	<.001	0.94
		LM	4.32	<.001	0.82
	Biphasic	PA	4.66	<.001	0.88
		LM	3.96	.006	0.75

current findings further. The same statistical approach described for the planned ones was applied if not otherwise specified.

3.2.1 | Influence of decay in monophasic PA and LM conditions

Visual inspection of TEP topographies (Figure 2a,b) and data on M1-P15 from the registered analyses suggested that this component's amplitude was lower in monophasic PA and LM conditions concerning the other four experimental conditions. However, we considered the possibility that a residual decay artefact in these two conditions could affect the results. Therefore, we conducted an additional qualitative analysis in these conditions to verify if a clearer M1-P15 could be identified after reducing the possible effect of the residual decay artefact.

For this, we re-run the pipeline for TEP preprocessing previously described in Section 2.6, to which we added the identification and removal of ICA components related to decay artefacts in the step for the selection and rejection of the components linked to vertical and horizontal ocular movements. All other preprocessing steps were unchanged. The components related to ocular movements were unchanged as they were still identified within the weight matrix obtained previously in the main analysis. The following steps of the pipeline were the same as described in the preprocessing section, and the same SSP-SIR components and artefactual trials were selected and removed. At the end of preprocessing, the grand averages of the two experimental conditions were obtained, and the M1-P15 was identified as before (i.e. between 7 and 25 ms); then, this component was visually compared with the one obtained in the same conditions using the preregistered pipeline.

This exploratory analysis highlighted that removing the residual decay artefact did not substantially change TEP topography (Figure 7a) and confirmed a relatively small M1-P15 amplitude, similar to preregistered analyses (Figure 2a). Therefore, it is unlikely that M1-P15 differences in monophasic PA and LM conditions may be due to the presence of residual decay artefacts in the EEG signal.

3.2.2 | Effects of TMS intensity on M1-P15 amplitude

To further understand the effects of TMS parameters on M1-P15, we considered the possibility that the modulations of M1-P15 amplitude found in the registered analyses could be partly explained by differences in TMS intensity across conditions. Indeed, the stimulation intensity was adjusted based on the rMT of that specific condition. Hence, we run two analyses of covariance (ANCOVA), one for each pulse waveform, with factor 'Current direction' (PA, AP, LM), and covarying the TMS intensity used to record it. This strategy allowed us to overcome the possible difference in the magnitude of the stimulator output, considering that we exploited two different machines.

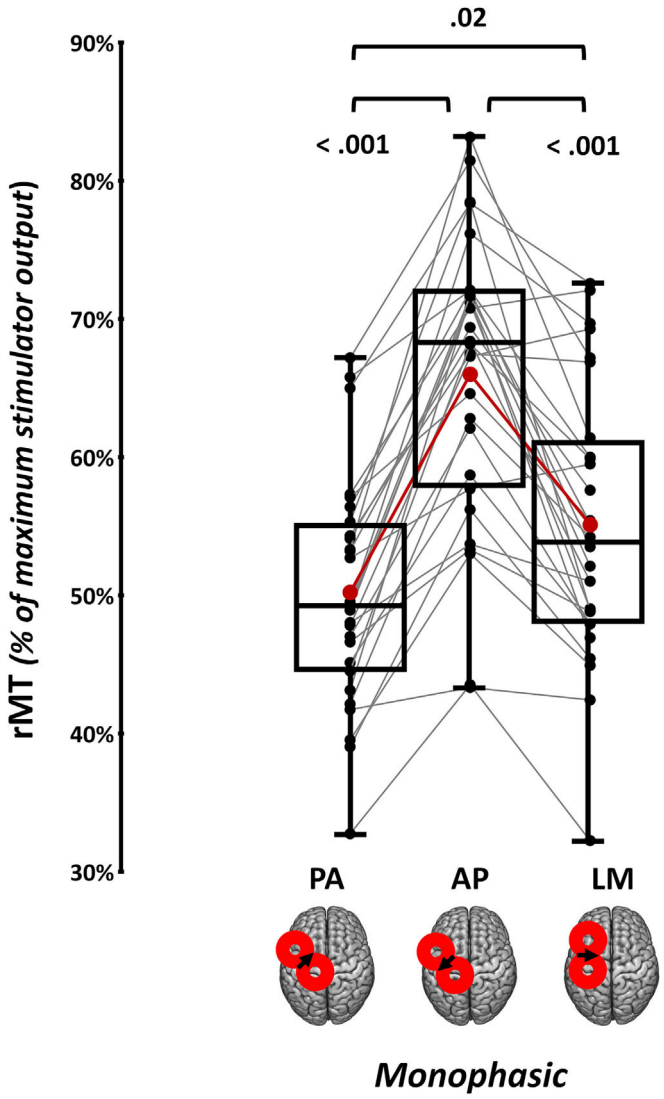

FIGURE 6 Positive control. rMT values obtained in monophasic conditions. Black arrows depicted over the stylized TMS coils indicate the direction of the current induced in M1. In box-and-whiskers plots, red dots and red lines indicate 20% trimmed means of the distributions, and the centre line denotes their median values. Black dots and grey lines show individual participants' scores. The box contains the 25th to 75th percentiles of the dataset. Whiskers extend to the largest observation, which falls within the 1.5 times inter-quartile range from the first/third quartile; significant *p* values of corrected post-hoc comparisons are reported.

The ANCOVA conducted on monophasic conditions confirmed the effect of the current direction found in the registered analysis by showing a significant effect of 'Current direction' ($F_{2,80} = 20.52$, $p < .001$, $\eta_p^2 = .339$) and no statistically significant effect of the covariate 'Stimulation intensity' ($F_{1,80} = 1.94$, $p = .167$, $\eta_p^2 = .024$). In detail, AP direction led to higher M1-P15 amplitude than PA ($t_{80} = 5.49$, $p < .001$) and LM ones ($t_{80} = 5.98$, $p < .001$)—that is, the same pattern found in the main analyses. This result corroborated the pattern found in M1-P15 amplitude from the main analysis (Figure 3a, left panel). It shows that differences in amplitude are unrelated to higher (or lower) stimulation intensity used in the different monophasic conditions.

The ANCOVA conducted on biphasic conditions showed no statistically significant effect of 'Current direction' ($F_{2,80} = 1.76$, $p = .178$, $\eta_p^2 = .042$) and a significant effect of the covariate 'Stimulation intensity' ($F_{2,80} = 6.4$, $p = .013$, $\eta_p^2 = .074$). Namely, regardless of the induced current direction, M1-P15 amplitude recorded with biphasic pulse waveform tended to increase as stimulation intensity increased. Still, no statistically significant modulation of current directions was observed, keeping this effect under control. This evidence suggests that the significant effect found in the main analysis between biphasic PA and LM conditions (Figure 3a, right panel) is likely due to the different stimulation intensities used in these two conditions (i.e. higher stimulation intensity in the LM condition; see Supplementary Materials – rMT in biphasic conditions).

3.2.3 | Spatial correlation between PA biphasic with the ipsilateral hand contracted and the other ones

Our preregistered analyses showed that amplitude and latency of M1-P15 were scarcely reproducible when TMS parameters were changed compared to the reference condition, that is, biphasic PA stimulation with ipsilateral hand contraction. These analyses considered data extracted from the electrode pair corresponding to the M1-P15 peak and do not inform on the topographical similarity between conditions. Here, we further explored similarity by calculating spatial correlations following the same procedure described by Conde et al. (2019) and Bertazzoli et al. (2021). At each time point, we correlated the voltage of all the electrodes in each condition pairs—that is, the condition with ipsilateral hand contraction and each condition with relaxed hands—with pairwise Spearman correlation (Bertazzoli et al., 2021; Conde et al., 2019).

Results showed that topography of TEPs in the biphasic PA condition with ipsilateral hand contraction was highly correlated with topography in the biphasic PA condition with the relaxed ipsilateral hand and with topography in the biphasic AP condition (*Spearman's rho* = .6–.9), followed by moderate correlation with biphasic LM and monophasic AP (*Spearman's rho* = .4–.6) and finally by weak correlations with monophasic LM and monophasic PA (*Spearman's rho* = .1–.3)

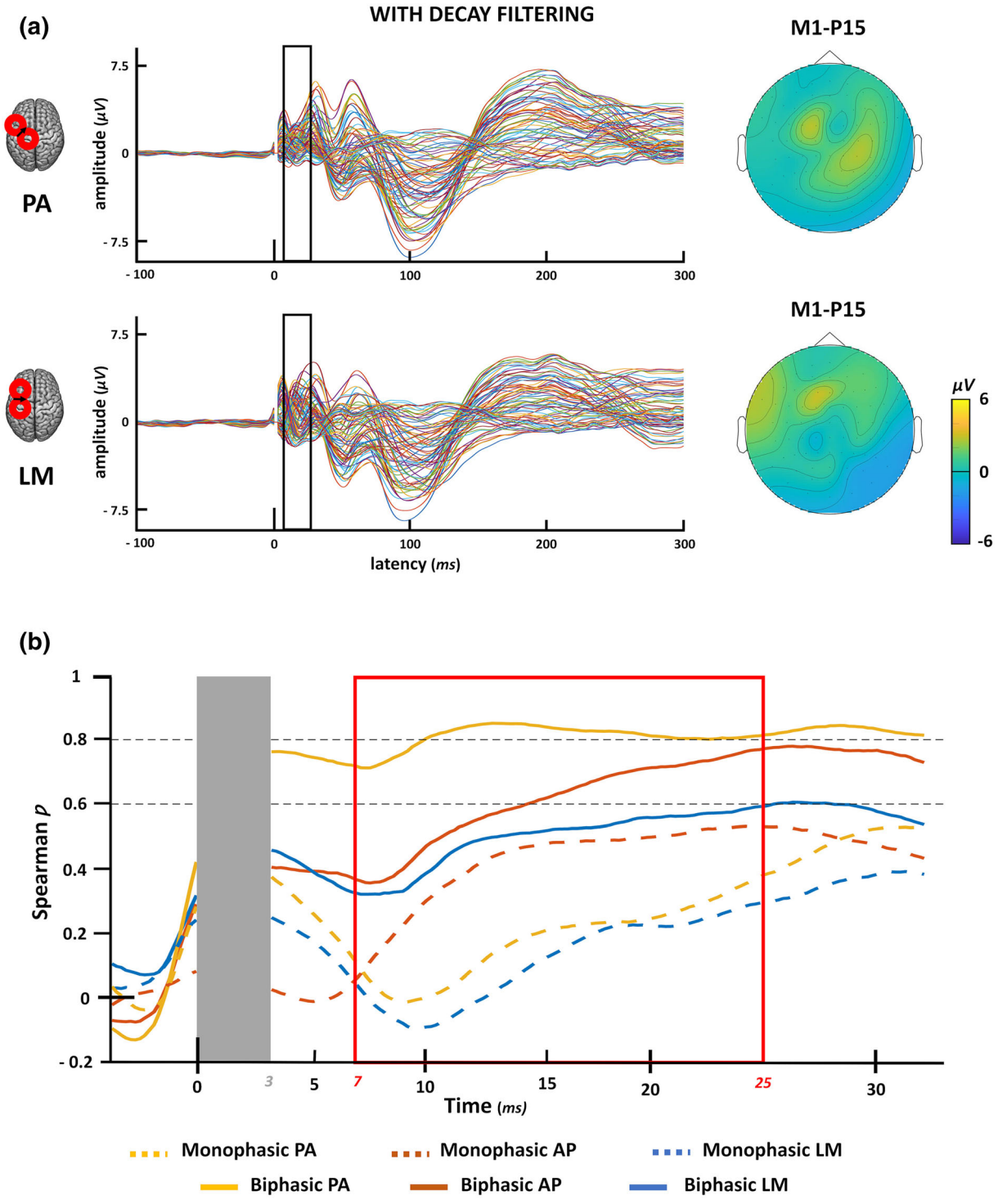

FIGURE 7 Effects of decay and M1-P15 spatial correlation. (a) Grand average of TEPs (left panel) and related topography of the M1-P15 between 7 and 25 ms (right panel) recorded in monophasic PA and monophasic LM conditions by taking into account for decay artefacts during the rejection of ICA components. M1-P15 was extracted by pooling electrodes F4 and FC4. M1-P15 topography maps used the same amplitude window of Figure 2a. (b) M1-P15 spatial correlation. Each line represents the spatial correlation (y-axis) over time (x-axis) of the experimental condition with the biphasic PA condition where participants have the ipsilateral hand slightly contracted. The grey column around zero represents the TMS-pulse interpolation interval. The red window represents the time interval considered for M1-P15 extraction (i.e. 7–25 ms). Horizontal dotted lines represent the threshold for moderate (.6) and substantial (.8) correlation.

(Figure 7b). These results are consistent with findings on the reliability and agreement measures on the peaks, suggesting that the conditions showing high reliability are also highly correlated in their topographical pattern. In contrast, conditions with low reliability present varied topographical patterns and low spatial consistency.

3.2.4 | Reliability and agreement of M1-P15 in participants with a clear M1-P15 peak

In this analysis, we explored if cases in which the M1-P15 peak could not be identified could impact the reliability of M1-P15, as they could be associated with higher measurement errors. In a few participants and conditions, the maximum value was at one edge of the predefined time window (i.e. at 7 or 25 ms, Figure S1). We explored the ICC and CCC indexes after excluding these cases for each pair of conditions, that is, the biphasic PA condition with the contracted ipsilateral hand and the other six experimental conditions (Table 3). Regarding the ICC, results confirmed good reliability between biphasic PA with the contracted ipsilateral hand and the same stimulation condition with the ipsilateral hand relaxed for the M1-P15 amplitude (ICC = .773), consistent with the analyses on the whole sample. Interestingly, latency for the same pair of conditions reached moderate reliability (ICC = .718; Koo & Li, 2016). Moreover, moderate reliability was also observed with the latency of the monophasic PA direction (ICC = .534). The same pattern was found for CCC ($PA_{biphasic}$ amplitude: CCC = .764; $PA_{biphasic}$ latency: CCC = .705; $PA_{monophasic}$ latency: CCC = .512, Figure 8a). All the other comparisons confirmed poor reliability and agreement (all ICC and CCC values <.5).

3.2.5 | Relation between normalized iSP area and M1-P15 amplitude

As we exploited the biphasic PA condition with the contracted ipsilateral hand as a reference condition to measure M1-P15 based on previous studies, we aimed at replicating findings that support its inter-hemispheric origin, that is, the positive relationship between M1-P15 amplitude and the normalized iSP area (Bortoletto et al., 2021; Zazio et al., 2022). MEPs from the left-hand APB muscle were preprocessed following the EMG pipeline described in Sections 2.6 and 2.7. iSP parameters were assessed in the trace obtained by averaging the rectified EMG traces recorded during the TMS-EEG block of the biphasic PA condition with the ipsilateral hand contracted. The following iSP parameters were considered: the iSP onset, defined as the point after cortical stimulation at which EMG activity constantly became (for a minimum duration of 10 ms) below the mean amplitude of EMG activity preceding the cortical stimulus; the iSP duration, calculated by subtracting the onset time from the ending time (i.e. the first point after iSP onset at which the level of EMG activity returned to the mean EMG signal); and the normalized iSP area, calculated using the following formula: [(area of the rectangle defined as mean EMG × iSP duration) − (area underneath the iSP)]. Then, the normalized iSP area was defined as the ratio between the iSP area and the area underneath EMG from −150 to 50 ms preceding TMS and multiplied by 100 (for a similar procedure, see Bortoletto et al., 2021; Zazio et al., 2022). Simple linear regression was used to test if the normalized iSP predicted M1-P15 amplitude.

The overall linear regression model was statistically significant ($F_{1,27} = 4.81$, $p = .037$, $R^2 = .156$). The fitted regression was: 'M1-P15 amplitude = 3.16 + 24.01*

TABLE 3 ICC and CCC values obtained excluding participants without a clear peak (i.e. M1-P15 latency fall at the edges of our selected time windows) by comparing each M1-P15 latency and amplitude recorded in the six main experimental blocks with the ones recorded in the block replicating the parameters used in the previous studies of our research group (Bortoletto et al., 2021; Zazio et al., 2022).

[no participants without a clear peak] Biphasic PA direction with ipsilateral hand contracted ($n = 22$) versus		N in common	Amplitude		Latency	
			ICC	CCC	ICC	CCC
Biphasic	PA ($n = 22$)	19	**.773**	**.764**	**.718**	**.705**
	AP ($n = 18$)	14	.123	.207	.139	.291
	LM ($n = 25$)	20	.059	.206	.424	.403
Monophasic	PA ($n = 18$)	16	.191	.176	**.534**	**.512**
	AP ($n = 16$)	13	−.416	−.014	.2	.174
	LM ($n = 26$)	21	.345	.324	.259	.245

Note: Values in bold indicate moderate (>.5) and good (>.75) reliability (for ICC) or agreement (for CCC).

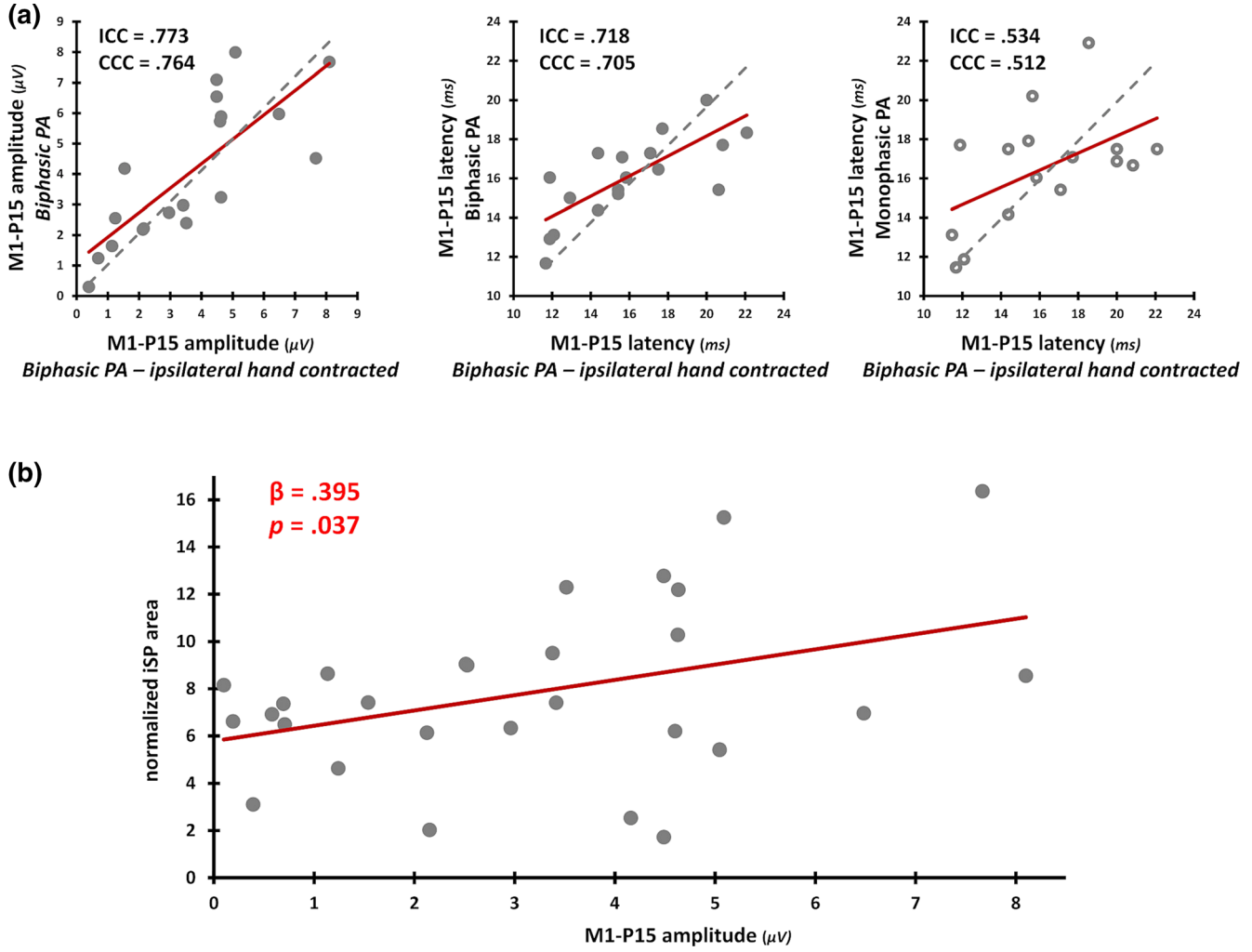

FIGURE 8 ICC and CCC removing outliers and M1-P15-iSP area relationship. (a) Concordance plots for moderate and good ICC and CCC values removing participants in which M1-P15 was identified at the edges of the time window that we considered for its extraction (i.e. 7–25 ms). *First two plots:* concordance plots for M1-P15 amplitude and latency between blocks where TMS is delivered exploiting biphasic PA current direction (one with the participant's ipsilateral hand relaxed and the other with the ipsilateral hand contracted). *Third plot*: concordance plot for M1-P15 latency between the block exploiting monophasic PA current direction and the one exploiting biphasic PA direction with the ipsilateral hand contracted. Dotted grey line: expected regression line if the two measures were perfectly correlated. Straight red line: actual regression line. It has to be noted that our ICC estimation does not take measurement error into account. (b) Positive significant relationship between M1-P15 amplitude and normalized iSP area, recorded in the experimental condition replicating the parameters exploited in our previous studies on this TEP component (Bortoletto et al., 2021; Zazio et al., 2022).

(normalized iSP area)', showing that the normalized iSP area is significantly predicted by M1-P15 amplitude ($\beta = .395$, $p = .037$; Figure 8b). Namely, the greater the iSP area, the greater the amplitude of the M1-P15 component, thus replicating the pattern of results already found in our previous studies on such a TEP component (Bortoletto et al., 2021; Zazio et al., 2022).

4 | DISCUSSION

Our study investigated the impact of two critical TMS parameters, that is, TMS pulse waveform and direction of the induced currents in the brain, on an early TEP component possibly reflecting inter-hemispheric cortico-cortical connectivity, namely, the M1-P15 (Bortoletto et al., 2021; Zazio et al., 2022). The aim was to address the current need to understand sources of TEP variability (*a*) for developing inter-hemispheric connectivity-based biomarkers in pathological conditions involving corpus callosum alterations and asymmetrical pathology as in psychiatric disorders (for a review, see Cao et al., 2021), like major depressive disorder (Cotovio et al., 2022; Dhami et al., 2021; Voineskos et al., 2019), schizophrenia (Ferrarelli et al., 2019; McKenna et al., 2020; Noda et al., 2018; Radhu et al., 2015), or dementia (Bagattini

et al., 2019; Julkunen et al., 2011; Lubben et al., 2021; Nardone et al., 2021); and (*b*) for the investigation of inter-hemispheric connectivity in general.

Overall, our results showed that pulse waveform and current direction are crucial parameters to evoke the M1-P15 (influencing both its amplitude and latency) and obtain stable and reliable measurements. Our study highlights how these parameters can affect early TEPs and suggests that they may introduce variability of outcomes across individuals and studies if not adequately controlled.

First, M1-P15 amplitude was strongly affected by the current direction in monophasic stimulation. The M1-P15 was not generated in two monophasic conditions, namely, PA and LM stimulation. In these conditions, the amplitude was lower than any other condition in the experiment, and the topography of the potential on the scalp was scarcely correlated with the typical topography of the M1-P15. Even a more tailored preprocessing to remove a residual decay artefact did not substantially modify the characteristics of the evoked potentials in these conditions. Differently, the monophasic AP direction generated the highest amplitude among the experimental conditions. With biphasic pulses, differences in M1-P15 amplitude were found between LM and PA current directions. Differences were also found when comparing the same current direction exploiting different pulse waveforms. Specifically, PA and LM current directions had higher M1-P15 amplitude for biphasic than monophasic stimulation, whereas AP had higher M1-P15 for monophasic than biphasic stimulation. It is important to consider that stimulation intensity in each experimental condition was adjusted to the corresponding rMT and therefore was different across conditions. This is a standard procedure in TMS and TMS-EEG studies targeting M1 wherein stimulation intensity is based on the individual's corticospinal excitability, that is, rMT (Hernandez-Pavon et al., 2023). When TEPs are recorded, it is assumed that rMT well represents both corticospinal and cortical excitability—namely, that rMT will adjust MEPs and TEPs in the same way. In our study, adjusting stimulation intensity based on the participant's rMT (i.e. stimulating at the 110% of such a value) equalized responses of the corticospinal tract, as indicated by non-significant modulation of $\log_{10}$ MEP amplitude across conditions. However, this procedure did not equalize responses of cortico-cortical tracts, as indicated by the statistically significant modulation found for M1-P15 amplitude. These results suggest that the excitability of the corticospinal tract may not correspond to the excitability of other cortico-cortical circuits in which the target region is embedded. Therefore, during TMS-EEG, personalizing TMS intensity based on rMT may not be sufficient for studying cortico-cortical effective connectivity, even for M1 stimulation (Saari et al., 2018).

Interestingly, stimulation intensity did not fully explain modulations of M1-P15 amplitude for the current direction. When stimulation intensity was controlled in the explorative analyses (see Section 3.2.2), the current direction did not affect M1-P15 amplitude in biphasic conditions as in monophasic conditions. We can hypothesize that with biphasic waveforms, and, at least for cortical responses, each phase of the stimulator's output induces a physiologically significant tissue current (e.g. Corthout et al., 2001), activating the population of intratelencephalic neurons responsible for cortico-cortical connectivity. Therefore, a biphasic pulse waveform may be more appropriate for recording early TEP components. Furthermore, at variance with other studies that investigate the spatio-temporal profile of TEPs (Bonato et al., 2006; Casula et al., 2018), our results did not show that pulse waveform or current direction can affect the polarity of early components. Namely, in all our conditions, M1-P15 was always found as a positive peak, despite differences in the topographical pattern. However, compared with previous studies, we analysed EEG responses earlier than 20 ms after the TMS pulse.

M1-P15 latency was modulated by TMS parameters too. The AP current direction for monophasic and biphasic pulses evoked a component peaking around 20–21 ms, significantly later than the peaks in PA and LM conditions (around 15–17 ms). This result aligns with a previous study from our group (Zazio et al., 2021), in which we employed biphasic AP stimulation and recorded a component with the same features as the M1-P15 but with latency over 20 ms, which we called P25. This component was localized in the motor area contralateral to the stimulation and was positively associated with pre-stimulus inter-hemispheric phase synchronization in the alpha band (Zazio et al., 2021). Interestingly, the present study shows delayed latency in AP condition both for M1-P15 and for MEPs—the latter result, as expected from previous literature (e.g. Davila-Pérez et al., 2018; Di Lazzaro et al., 2001; D'Ostilio et al., 2016; Sommer et al., 2006). Considering cortico-cortical connectivity, we can hypothesize that AP current direction activates different neuronal populations than PA and LM in the superficial layers of M1, as already highlighted for the cortico-spinal tract (McColgan et al., 2020; Spampinato, 2020). Indeed, it has been suggested that AP direction activates a more anterior portion of the precentral gyrus than PA, corresponding to the caudal premotor area (Aberra et al., 2020; Siebner et al., 2022). This region is strongly interconnected with the ipsilateral and the contralateral M1 (Spampinato, 2020). Therefore, AP stimulation may delay

M1-P15 latency because it activates an indirect pathway, including the targeted premotor area, the ipsilateral M1, and the contralateral motor areas. This observation is consistent with the known excitatory connection, which typically takes 1–6 ms to activate M1 neurons following stimulation of the ipsilateral premotor cortex (Ghosh & Porter, 1988; Groppa, Schlaak, et al., 2012; Parmigiani et al., 2018). Hence, given the direct inter-hemispheric connection between the premotor cortex and the contralateral M1, AP stimulation may activate this alternative route.

The replicability of M1-P15 amplitude and latency was negatively affected by TMS parameters, suggesting that these factors need to be controlled to obtain stable measures at a single subject level. Poor replicability across stimulation conditions may further support that TMS parameters determine the neural population that is preferentially targeted, even when the hotspot is unchanged. Noteworthy, the replicability of M1-P15 amplitude was good for the same stimulation conditions, even if they differed for ipsilateral hand contraction. Similarly, previous studies have reported substantial reliability (Zazio et al., 2021) and strong correlation (Lioumis et al., 2009) of amplitude across sessions for early TEPs recorded after M1 stimulation. Moreover, no statistically significant differences have been found for M1-P15 amplitude and latency between the contracted and the relaxed ipsilateral hand (Zazio et al., 2022). Therefore, these data suggest that M1-P15 amplitude can be measured with high stability at a single subject level and meet crucial criteria for developing cortico-cortical connectivity-based biomarkers (Julkunen et al., 2022; Parmigiani et al., 2022), provided the same TMS parameters of the original studies (Bortoletto et al., 2021; Zazio et al., 2022). Further studies will be needed to understand if these results can be generalized to different target areas and other TEP components, as previous works have reported inconsistencies in replicability (de Goede et al., 2020; Kerwin et al., 2018), which may also depend on signal preprocessing (Bertazzoli et al., 2021). Therefore, careful methodological choices are needed to collect reproducible signals (Hernandez-Pavon et al., 2022). Differently from amplitude, the latency of M1-P15 showed low replicability even in the same stimulation condition. Latency is likely more prone to residual artefacts and residual noise in general. By removing participants whose latency value was at the edge of the window of interest as they did not show a clear peak, reliability and agreement of latency improved and reached moderate values (see Section 3.2.4). This exploratory analysis highlights the need for further improvement of the TMS-EEG technique to obtain stable values of early latencies in each subject.

As said, M1-P15 may reflect the interhemispheric inhibition of the motor areas contralateral to TMS via the corpus callosum (Bortoletto et al., 2021; Zazio et al., 2022) hence offering an excellent benchmark to explore cortico-cortical connectivity without the mediation of peripheral corticospinal measures. Our results further corroborate the contralateral origin of M1-P15 after activation of inter-hemispheric connections. First, we replicated the positive relationship between M1-P15 amplitude and iSP area (see Section 3.2.5), which we already reported in two previous studies (Bortoletto et al., 2021; Zazio et al., 2022). Second, we found patterns of M1-P15 modulation that align with effects reported on iSP in previous literature. Specifically, it is interesting to consider the monophasic conditions in which M1-P15 was not generated, that is, PA and LM. For instance, Chen et al. (2003) found that iSP obtained with monophasic PA direction has a higher recording threshold (expressed as a ratio of the active MT) than the one registered with the AP direction, suggesting that, with this coil orientation, intratelencephalic neurons responsible for M1-to-M1 connectivity are more difficult to activate concerning corticospinal tract ones (Chen et al., 2003). Different studies using a Magstim 200 stimulator (i.e. the same model used in the present work for monophasic conditions) have indeed shown that the intensity to produce stable iSP values is around 80% MSO, a percentage greater than the average one exploited in our sample (see Figure 6) (e.g. Fleming & Newham, 2017; Jung et al., 2006; Jung & Ziemann, 2006; Meyer et al., 1995). In the present study, iSP was recorded only in the condition replicating the parameters of our original studies, namely, biphasic PA (Bortoletto et al., 2021; Zazio et al., 2022). Future research may also record iSP with other coil orientations, thus shedding light on the results found for M1-P15 amplitude. The evidence that the pattern found for the LM direction is similar to the one found for PA suggests that LM activates, at least partially, the same neuronal populations of the latter direction. In this regard, it must be noted that, in terms of orientation, LM is closer to PA direction than AP (i.e. 90° orientation to the sagittal plane *versus* 45° for PA and 135° for AP).

Overall, our study points out the importance of considering TMS technical parameters as pulse waveform and induced current direction when early cortico-cortical TEP responses are recorded and, in a broader perspective, when TMS-EEG is used. Our results showed that these parameters could critically modulate the magnitude and presence of early components like the M1-P15 in the recorded TEPs. Indeed, at variance with MEPs, M1-P15 amplitude seems crucially affected by the stimulator's pulse waveform. When monophasic waveforms are exploited, the direction of currents induced in the brain

tissue is critical for successfully recording the M1-P15. Conversely, its latency is mainly influenced by the current direction. Like MEPs, the AP direction led to higher values than the other two directions exploited, regardless of the pulse waveform used to record it. The importance of stimulation parameters is confirmed by the evidence that this component shows low replicability across conditions, at least when different parameters than the original ones (i.e. biphasic waveform and PA direction) are used. Hence, future studies should carefully consider the effects of stimulator parameters on early TEP components like the M1-P15 and extend such an investigation to other cortical areas, especially if TEPs will be used as potential biomarkers of healthy and pathological effective connectivity.

AUTHOR CONTRIBUTIONS

Giacomo Guidali: Conceptualization, methodology, investigation, data curation, software, formal analysis, visualization, writing—original draft. **Agnese Zazio**: Conceptualization, methodology, software, formal analysis, validation, visualization, writing—original draft. **Delia Lucarelli:** Investigation, software, formal analysis, writing—review and editing. **Eleonora Marcantoni**: Investigation, software, writing—review and editing. **Antonietta Stango:** Software, formal analysis, writing—review and editing. **Guido Barchiesi:** Software, writing—review and editing. **Marta Bortoletto:** Conceptualization, data curation, funding acquisition, methodology, resources, supervision, project administration, writing—original draft.

ACKNOWLEDGEMENTS

We would like to thank Claudia Fracassi for her precious technical assistance. Open access funding provided by BIBLIOSAN.

CONFLICT OF INTEREST STATEMENT

The authors declare that the research was conducted in the absence of any commercial or financial relationships that could be construed as a potential conflict of interest.

PEER REVIEW

The peer review history for this article is available at https://www.webofscience.com/api/gateway/wos/peer-review/10.1111/ejn.16127.

DATA AVAILABILITY STATEMENT

Raw data, analysis dataset, code, and stimuli of the study are publicly available on G-Node: https://gin.g-node.org/Giacomo_Guidali/Guidali_et_al_2023_EJN_RR. Raw data, analysis dataset, code, and stimuli of the pilot experiment (see Supporting Information) are publicly available on Open Science Framework (OSF): https://osf.io/jrxq7/.

ORCID

Giacomo Guidali https://orcid.org/0000-0002-3741-0404
Agnese Zazio https://orcid.org/0000-0002-1395-9005
Delia Lucarelli https://orcid.org/0000-0001-5847-0572
Eleonora Marcantoni https://orcid.org/0000-0003-1137-4983
Antonietta Stango https://orcid.org/0000-0003-1387-2150
Guido Barchiesi https://orcid.org/0000-0002-8936-4171
Marta Bortoletto https://orcid.org/0000-0002-8489-8043

REFERENCES

Aberra, A. S., Wang, B., Grill, W. M., & Peterchev, A. V. (2020). Simulation of transcranial magnetic stimulation in head model with morphologically-realistic cortical neurons. *Brain Stimulation*, *13*(1), 175–189. https://doi.org/10.1016/J.BRS.2019.10.002

Anderson, S. F., Kelley, K., & Maxwell, S. E. (2017). Sample-size planning for more accurate statistical power: A method adjusting sample effect sizes for publication bias and uncertainty. *Psychological Science*, *28*(11), 1547–1562. https://doi.org/10.1177/0956797617723724

Awiszus, F. (2003). TMS and threshold hunting. *Supplements to Clinical Neurophysiology*, *56*(C), 13–23. https://doi.org/10.1016/S1567-424X(09)70205-3

Bagattini, C., Mutanen, T. P., Fracassi, C., Manenti, R., Cotelli, M., Ilmoniemi, R. J., Miniussi, C., & Bortoletto, M. (2019). Predicting Alzheimer's disease severity by means of TMS–EEG coregistration. *Neurobiology of Aging*, *80*, 38–45. https://doi.org/10.1016/j.neurobiolaging.2019.04.008

Barnhart, H. X., Lokhnygina, Y., Kosinski, A. S., & Haber, M. (2007). Comparison of concordance correlation coefficient and coefficient of individual agreement in assessing agreement. *Journal of Biopharmaceutical Statistics*, *17*(4), 721–738. https://doi.org/10.1080/10543400701329497

Barre, P. E., Redini, F., Boumediene, K., Vielpeau, C., & Pujol, J. P. (2001). Comparison of descending volleys evoked by monophasic and biphasic magnetic stimulation of the motor cortex in conscious humans. *Experimental Brain Research*, *141*(1), 121–127. https://doi.org/10.1007/s002210100863

Bertazzoli, G., Esposito, R., Mutanen, T. P., Ferrari, C., Ilmoniemi, R. J., Miniussi, C., & Bortoletto, M. (2021). The impact of artifact removal approaches on TMS–EEG signal. *NeuroImage*, *239*, 118272. https://doi.org/10.1016/J.NEUROIMAGE.2021.118272

Bestmann, S., & Krakauer, J. W. (2015). The uses and interpretations of the motor-evoked potential for understanding behaviour. *Experimental Brain Research*, *233*(3), 679–689. https://doi.org/10.1007/s00221-014-4183-7

Biabani, M., Fornito, A., Mutanen, T. P., Morrow, J., & Rogasch, N. C. (2019). Characterizing and minimizing the contribution of sensory inputs to TMS-evoked potentials. *Brain Stimulation*, *12*(6), 1537–1552. https://doi.org/10.1016/j.brs.2019.07.009

Bigoni, C., Cadic-Melchior, A., Vassiliadis, P., Morishita, T., & Hummel, F. C. (2022). An automatized method to determine latencies of motor-evoked potentials under physiological and

pathophysiological conditions. *Journal of Neural Engineering*, *19*(2), 024002. https://doi.org/10.1088/1741-2552/ac636c

Bonato, C., Miniussi, C., & Rossini, P. M. (2006). Transcranial magnetic stimulation and cortical evoked potentials: A TMS/EEG co-registration study. *Clinical Neurophysiology*, *117*(8), 1699–1707. https://doi.org/10.1016/j.clinph.2006.05.006

Bortoletto, M., Bonzano, L., Zazio, A., Ferrari, C., Pedullà, L., Gasparotti, R., Miniussi, C., & Bove, M. (2021). Asymmetric transcallosal conduction delay leads to finer bimanual coordination. *Brain Stimulation*, *14*, 379–388. https://doi.org/10.1016/j.brs.2021.02.002

Bortoletto, M., Veniero, D., Thut, G., & Miniussi, C. (2015). The contribution of TMS-EEG coregistration in the exploration of the human cortical connectome. *Neuroscience and Biobehavioral Reviews*, *49*, 114–124. https://doi.org/10.1016/j.neubiorev.2014.12.014

Cao, K. X., Ma, M. L., Wang, C. Z., Iqbal, J., Si, J. J., Xue, Y. X., & Yang, J. L. (2021). TMS-EEG: An emerging tool to study the neurophysiologic biomarkers of psychiatric disorders. *Neuropharmacology*, *197*, 108574. https://doi.org/10.1016/J.NEUROPHARM.2021.108574

Carrasco, J. L., & Jover, L. (2003). Estimating the generalized concordance correlation coefficient through variance components. *Biometrics*, *59*(4), 849–858. https://doi.org/10.1111/j.0006-341X.2003.00099.x

Casarotto, S., Romero Lauro, L. J., Bellina, V., Casali, A. G., Rosanova, M., Pigorini, A., Defendi, S., Mariotti, M., & Massimini, M. (2010). EEG responses to TMS are sensitive to changes in the perturbation parameters and repeatable over time. *PLoS ONE*, *5*(4), e10281. https://doi.org/10.1371/journal.pone.0010281

Casula, E. P., Rocchi, L., Hannah, R., & Rothwell, J. C. (2018). Effects of pulse width, waveform and current direction in the cortex: A combined cTMS-EEG study. *Brain Stimulation*, *11*(5), 1063–1070. https://doi.org/10.1016/j.brs.2018.04.015

Chen, R., Yung, D., & Li, J. Y. (2003). Organization of ipsilateral excitatory and inhibitory pathways in the human motor cortex. *Journal of Neurophysiology*, *89*(3), 1256–1264. https://doi.org/10.1152/JN.00950.2002/ASSET/IMAGES/LARGE/9K0332919007.JPEG

Comolatti, R., Pigorini, A., Casarotto, S., Fecchio, M., Faria, G., Sarasso, S., Rosanova, M., Gosseries, O., Boly, M., Bodart, O., Ledoux, D., Brichant, JF., Nobili, L., Laureys, S., Tononi, G., Massimini, M., & Casali, A. G. (2019). A fast and general method to empirically estimate the complexity of brain responses to transcranial and intracranial stimulations. *Brain Stimulation*, *12*(5), 1280–1289. https://doi.org/10.1016/j.brs.2019.05.013

Conde, V., Tomasevic, L., Akopian, I., Stanek, K., Saturnino, G. B., Thielscher, A., Bergmann, T. O., & Siebner, H. R. (2019). The non-transcranial TMS-evoked potential is an inherent source of ambiguity in TMS-EEG studies. *NeuroImage*, *185*, 300–312. https://doi.org/10.1016/j.neuroimage.2018.10.052

Corp, D. T., Bereznicki, H. G. K., Clark, G. M., Youssef, G. J., Fried, P. J., Jannati, A., Davies, C. B., Gomes-Osman, J., Kirkovski, M., Albein-Urios, N., Fitzgerald, P. B., Koch, G., di Lazzaro, V., Pascual-Leone, A., Enticott, P. G., & 'Big TMS Data Collaboration'. (2021). Large-scale analysis of interindividual variability in single and paired-pulse TMS data. *Clinical Neurophysiology*, *132*, 2639–2653. https://doi.org/10.1016/j.clinph.2021.06.014

Corthout, E., Barker, A. T., & Cowey, A. (2001). Transcranial magnetic stimulation: Which part of the current waveform causes the stimulation? *Experimental Brain Research*, *141*(1), 128–132. https://doi.org/10.1007/s002210100860

Cotovio, G., Rodrigues da Silva, D., Real Lage, E., Seybert, C., & Oliveira-Maia, A. J. (2022). Hemispheric asymmetry of motor cortex excitability in mood disorders – Evidence from a systematic review and meta-analysis. *Clinical Neurophysiology*, *137*, 25–37. https://doi.org/10.1016/J.CLINPH.2022.01.137

Davila-Pérez, P., Jannati, A., Fried, P. J., Cudeiro Mazaira, J., & Pascual-Leone, A. (2018). The effects of waveform and current direction on the efficacy and test-retest reliability of transcranial magnetic stimulation. *Neuroscience*, *393*, 97–109. https://doi.org/10.1016/j.neuroscience.2018.09.044

de Goede, A. A., Cumplido-Mayoral, I., & van Putten, M. J. A. M. (2020). Spatiotemporal dynamics of single and paired pulse TMS-EEG responses. *Brain Topography*, *33*(4), 425–437. https://doi.org/10.1007/s10548-020-00773-6

de Vet, H. C. W., Terwee, C. B., Knol, D. L., & Bouter, L. M. (2006). When to use agreement versus reliability measures. *Journal of Clinical Epidemiology*, *59*(10), 1033–1039. https://doi.org/10.1016/J.JCLINEPI.2005.10.015

Delignette-Muller, M. L., & Dutang, C. (2015). fitdistrplus: An R package for fitting distributions. *Journal of Statistical Software*, *64*(4), 1–34. https://doi.org/10.18637/jss.v064.i04

Delorme, A., & Makeig, S. (2004). EEGLAB: An open source toolbox for analysis of single-trial EEG dynamics including independent component analysis. *Journal of Neuroscience Methods*, *134*(1), 9–21. https://doi.org/10.1016/J.JNEUMETH.2003.10.009

Dhami, P., Atluri, S., Lee, J., Knyahnytska, Y., Croarkin, P. E., Blumberger, D. M., Daskalakis, Z. J., & Farzan, F. (2021). Neurophysiological markers of response to theta burst stimulation in youth depression. *Depression and Anxiety*, *38*(2), 172–184. https://doi.org/10.1002/DA.23100

Di Lazzaro, V., Oliviero, A., Profice, P., Ferrara, L., Saturno, E., Pilato, F., & Tonali, P. (1999). The diagnostic value of motor evoked potentials. *Clinical Neurophysiology*, *110*(7), 1297–1307. https://doi.org/10.1016/S1388-2457(99)00060-7

Di Lazzaro, V., Oliviero, A., Profice, P., Saturno, E., Pilato, F., Insola, A., Mazzone, P., Tonali, P., & Rothwell, J. C. (1998). Comparison of descending volleys evoked by transcranial magnetic and electric stimulation in conscious humans. *Electroencephalography and Clinical Neurophysiology - Electromyography and Motor Control*, *109*(5), 397–401. https://doi.org/10.1016/S0924-980X(98)00038-1

Di Lazzaro, V., Oliviero, A., Saturno, E., Pilato, F., Insola, A., Mazzone, P., Profice, P., Tonali, P., & Rothwell, J. (2001). The effect on corticospinal volleys of reversing the direction of current induced in the motor cortex by transcranial magnetic stimulation. *Experimental Brain Research*, *138*(2), 268–273. https://doi.org/10.1007/s002210100722

Di Lazzaro, V., Profice, P., Ranieri, F., Capone, F., Dileone, M., Oliviero, A., & Pilato, F. (2012). I-wave origin and modulation. *Brain Stimulation*, *5*(4), 512–525. https://doi.org/10.1016/j.brs.2011.07.008

Di Lazzaro, V., Rothwell, J., & Capogna, M. (2018). Noninvasive stimulation of the human brain: Activation of multiple cortical

circuits. *The Neuroscientist*, *24*(3), 246–260. https://doi.org/10.1177/1073858417717660

Di Lazzaro, V., & Ziemann, U. (2013). The contribution of transcranial magnetic stimulation in the functional evaluation of microcircuits in human motor cortex. *Frontiers in Neural Circuits*, *7*, 18. https://doi.org/10.3389/fncir.2013.00018

Dissanayaka, T., Zoghi, M., Farrell, M., Egan, G., & Jaberzadeh, S. (2018). Comparison of Rossini–Rothwell and adaptive threshold-hunting methods on the stability of TMS induced motor evoked potentials amplitudes. *Journal of Neuroscience Research*, *96*(11), 1758–1765. https://doi.org/10.1002/jnr.24319

D'Ostilio, K., Goetz, S. M., Hannah, R., Ciocca, M., Chieffo, R., Chen, J. C. A., Peterchev, A. V., & Rothwell, J. C. (2016). Effect of coil orientation on strength-duration time constant and I-wave activation with controllable pulse parameter transcranial magnetic stimulation. *Clinical Neurophysiology*, *127*(1), 675–683. https://doi.org/10.1016/j.clinph.2015.05.017

Faul, F., Erdfelder, E., Buchner, A., & Lang, A. G. (2009). Statistical power analyses using G*power 3.1: Tests for correlation and regression analyses. *Behavior Research Methods*, *41*(4), 1149–1160. https://doi.org/10.3758/BRM.41.4.1149

Ferrarelli, F., Kaskie, R. E., Graziano, B., Reis, C. C., & Casali, A. G. (2019). Abnormalities in the evoked frontal oscillatory activity of first-episode psychosis: A TMS/EEG study. *Schizophrenia Research*, *206*, 436–439. https://doi.org/10.1016/J.SCHRES.2018.11.008

Fleming, M. K., & Newham, D. J. (2017). Reliability of transcallosal inhibition in healthy adults. *Frontiers in Human Neuroscience*, *10*, 681. https://doi.org/10.3389/FNHUM.2016.00681/BIBTEX

George, D., & Mallery, P. (2019). *IBM SPSS statistics 26 step by step: A simple guide and reference*. Routledge. https://doi.org/10.4324/9780429056765

Ghosh, B. Y. S., & Porter, R. (1988). Corticocortical synaptic influences on morphologically identified pyramidal neurones in the motor cortex of the monkey. *The Journal of Physiology*, *400*, 617–629. https://doi.org/10.1113/jphysiol.1988.sp017139

Groppa, S., Oliviero, A., Eisen, A., Quartarone, A., Cohen, L. G., Mall, V., Kaelin-Lang, A., Mima, T., Rossi, S., Thickbroom, G. W., Rossini, P. M., Ziemann, U., Valls-Solé, J., & Siebner, H. R. (2012). A practical guide to diagnostic transcranial magnetic stimulation: Report of an IFCN committee. *Clinical Neurophysiology*, *123*(5), 858–882. https://doi.org/10.1016/j.clinph.2012.01.010

Groppa, S., Schlaak, B. H., Münchau, A., Werner-Petroll, N., Dünnweber, J., Bäumer, T., van Nuenen, B. F. L., & Siebner, H. R. (2012). The human dorsal premotor cortex facilitates the excitability of ipsilateral primary motor cortex via a short latency cortico-cortical route. *Human Brain Mapping*, *33*(2), 419–430. https://doi.org/10.1002/hbm.21221

Hamada, M., Galea, J. M., Di Lazzaro, V., Mazzone, P., Ziemann, U., & Rothwell, J. C. (2014). Two distinct interneuron circuits in human motor cortex are linked to different subsets of physiological and behavioral plasticity. *Journal of Neuroscience*, *34*(38), 12837–12849. https://doi.org/10.1523/JNEUROSCI.1960-14.2014

Harris, K. D., & Shepherd, G. M. G. (2015). The neocortical circuit: Themes and variations. *Nature Neuroscience*, *18*(2), 170–181. https://doi.org/10.1038/nn.3917

Hernandez-Pavon, J. C., Kugiumtzis, D., Zrenner, C., Kimiskidis, V. K., & Metsomaa, J. (2022). Removing artifacts from TMS-evoked EEG: A methods review and a unifying theoretical framework. *Journal of Neuroscience Methods*, *376*, 109591. https://doi.org/10.1016/j.jneumeth.2022.109591

Hernandez-Pavon, J. C., Veniero, D., Bergmann, T. O., Belardinelli, P., Bortoletto, M., Casarotto, S., Casula, E. P., Farzan, F., Fecchio, M., Julkunen, P., Kallioniemi, E., Lioumis, P., Metsomaa, J., Miniussi, C., Mutanen, T. P., Rocchi, L., Rogasch, N. C., Shafi, M. M., Siebner, H. R., … Ilmoniemi, R. J. (2023). TMS combined with EEG: Recommendations and open issues for data collection and analysis. *Brain Stimulation*, *16*(2), 567–593. https://doi.org/10.1016/J.BRS.2023.02.009

Hui, J., Tremblay, S., & Daskalakis, Z. J. (2019). The current and future potential of transcranial magnetic stimulation with electroencephalography in psychiatry. *Clinical Pharmacology and Therapeutics*, *106*(4), 734–746. https://doi.org/10.1002/cpt.1541

Julkunen, P., Jauhiainen, A. M., Knnen, M., Pääkknen, A., Karhu, J., & Soininen, H. (2011). Combining transcranial magnetic stimulation and electroencephalography may contribute to assess the severity of Alzheimer's disease. *International Journal of Alzheimer's Disease*, *2011*, 654794. https://doi.org/10.4061/2011/654794

Julkunen, P., Kimiskidis, V. K., & Belardinelli, P. (2022). Bridging the gap: TMS-EEG from lab to clinic. *Journal of Neuroscience Methods*, *369*, 109482. https://doi.org/10.1016/j.jneumeth.2022.109482

Jung, P., Beyerle, A., Humpich, M., Neumann-Haefelin, T., Lanfermann, H., & Ziemann, U. (2006). Ipsilateral silent period: A marker of callosal conduction abnormality in early relapsing–remitting multiple sclerosis? *Journal of the Neurological Sciences*, *250*(1–2), 133–139. https://doi.org/10.1016/J.JNS.2006.08.008

Jung, P., & Ziemann, U. (2006). Differences of the ipsilateral silent period in small hand muscles. *Muscle & Nerve*, *34*(4), 431–436. https://doi.org/10.1002/MUS.20604

Kammer, T., Beck, S., Erb, M., & Grodd, W. (2001). The influence of current direction on phosphene thresholds evoked by transcranial magnetic stimulation. *Clinical Neurophysiology*, *112*(11), 2015–2021. https://doi.org/10.1016/S1388-2457(01)00673-3

Kammer, T., Beck, S., Thielscher, A., Laubis-Hermann, U., & Topka, H. (2001). Motor threshold in humans: A transcranial magnetic stimulation study comparing different pulse waveforms, current directions and stimulator types. *Clinical Neurophysiology*, *112*, 250–258. https://doi.org/10.1016/S1388-2457(00)00513-7

Kerwin, L. J., Keller, C. J., Wu, W., Narayan, M., & Etkin, A. (2018). Test-retest reliability of transcranial magnetic stimulation EEG evoked potentials. *Brain Stimulation*, *11*(3), 536–544. https://doi.org/10.1016/J.BRS.2017.12.010

King, T. S., Chinchilli, V. M., & Carrasco, J. L. (2007). A repeated measures concordance correlation coefficient. *Statistics in Medicine*, *26*(16), 3095–3113. https://doi.org/10.1002/SIM.2778

Koch, G. (2020). Cortico-cortical connectivity: The road from basic neurophysiological interactions to therapeutic applications. *Experimental Brain Research*, *238*, 1677–1684. https://doi.org/10.1007/s00221-020-05844-5

Koo, T. K., & Li, M. Y. (2016). A guideline of selecting and reporting intraclass correlation coefficients for reliability research. *Journal of Chiropractic Medicine*, *15*(2), 155–163. https://doi.org/10.1016/j.jcm.2016.02.012

Lin, L. I. (1989). A concordance correlation coefficient to evaluate replicability. *Biomatrics*, *45*(1), 255–268. https://doi.org/10.2307/2532051

Lioumis, P., Kičić, D., Savolainen, P., Mäkelä, J. P., & Kähkönen, S. (2009). Replicability of TMS - evoked EEG responses. *Human Brain Mapping*, *30*(4), 1387–1396. https://doi.org/10.1002/hbm.20608

Lubben, N., Ensink, E., Coetzee, G. A., & Labrie, V. (2021). The enigma and implications of brain hemispheric asymmetry in neurodegenerative diseases. *Brain Communications*, *3*(3), fcab211. https://doi.org/10.1093/braincomms/fcab211

Maccabee, P. J., Nagarajan, S. S., Amassian, V. E., Durand, D. M., Szabo, A. Z., Ahad, A. B., Cracco, R. Q., Lai, K. S., & Eberle, L. P. (1998). Influence of pulse sequence, polarity and amplitude on magnetic stimulation of human and porcine peripheral nerve. *Journal of Physiology*, *513*(2), 571–585. https://doi.org/10.1111/j.1469-7793.1998.571bb.x

Mair, P., & Wilcox, R. (2020). Robust statistical methods in R using the WRS2 package. *Behavior Research Methods*, *52*(2), 464–488. https://doi.org/10.3758/s13428-019-01246-w

McColgan, P., Joubert, J., Tabrizi, S. J., & Rees, G. (2020). The human motor cortex microcircuit: Insights for neurodegenerative disease. *Nature Reviews Neuroscience*, *21*(8), 401–415. https://doi.org/10.1038/s41583-020-0315-1

McGraw, K. O., & Wong, S. P. (1996). Forming inferences about some intraclass correlation coefficients. *Psychological Methods*, *1*(1), 30–46. https://doi.org/10.1037/1082-989X.1.1.30

McKenna, F., Babb, J., Miles, L., Goff, D., & Lazar, M. (2020). Reduced microstructural lateralization in males with chronic schizophrenia: A diffusional kurtosis imaging study. *Cerebral Cortex*, *30*(4), 2281–2294. https://doi.org/10.1093/cercor/bhz239

Meyer, B. U., Röricht, S., Von Einsiedel, H. G., Kruggel, F., & Weindl, A. (1995). Inhibitory and excitatory interhemispheric transfers between motor cortical areas in normal humans and patients with abnormalities of the corpus callosum. *Brain*, *118*(2), 429–440. https://doi.org/10.1093/BRAIN/118.2.429

Momi, D., Ozdemir, R. A., Tadayon, E., Boucher, P., Shafi, M. M., Pascual-Leone, A., & Santarnecchi, E. (2021). Network-level macroscale structural connectivity predicts propagation of transcranial magnetic stimulation. *NeuroImage*, *229*, 117698. https://doi.org/10.1016/j.neuroimage.2020.117698

Mutanen, T. P., Kukkonen, M., Nieminen, J. O., Stenroos, M., Sarvas, J., & Ilmoniemi, R. J. (2016). Recovering TMS-evoked EEG responses masked by muscle artifacts. *NeuroImage*, *139*, 157–166. https://doi.org/10.1016/j.neuroimage.2016.05.028

Mutanen, T. P., Metsomaa, J., Liljander, S., & Ilmoniemi, R. J. (2018). Automatic and robust noise suppression in EEG and MEG: The SOUND algorithm. *NeuroImage*, *166*, 135–151. https://doi.org/10.1016/j.neuroimage.2017.10.021

Nardone, R., Sebastianelli, L., Versace, V., Ferrazzoli, D., Saltuari, L., & Trinka, E. (2021). TMS–EEG co-registration in patients with mild cognitive impairment, Alzheimer's disease and other dementias: A systematic review. *Brain Sciences 2021*, *11*, 303. https://doi.org/10.3390/BRAINSCI11030303

Noda, Y., Barr, M. S., Zomorrodi, R., Cash, R. F. H., Rajji, T. K., Farzan, F., Chen, R., George, T. P., Daskalakis, Z. J., & Blumberger, D. M. (2018). Reduced short-latency afferent inhibition in prefrontal but not motor cortex and its association with executive function in schizophrenia: A combined TMS-EEG study. *Schizophrenia Bulletin*, *44*(1), 193–202. https://doi.org/10.1093/SCHBUL/SBX041

Oldfield, R. C. (1971). The assessment and analysis of handedness: The Edinburgh inventory. *Neuropsychologia*, *9*(1), 97–113. https://doi.org/10.1016/0028-3932(71)90067-4

Oostenveld, R., Fries, P., Maris, E., & Schoffelen, J. M. (2011). FieldTrip: Open source software for advanced analysis of MEG, EEG, and invasive electrophysiological data. *Computational Intelligence and Neuroscience*, *2011*, 156869. https://doi.org/10.1155/2011/156869

Osborne, J. W. (2010). Improving your data transformations: Applying the Box-Cox transformation. *Practical Assessment, Research and Evaluation*, *15*(12).

Parmigiani, S., Ross, J. M., Cline, C. C., Minasi, C. B., Gogulski, J., & Keller, C. J. (2022). Reliability and validity of transcranial magnetic stimulation–electroencephalography biomarkers. *Biological Psychiatry: Cognitive Neuroscience and Neuroimaging.*, *8*, 805–814. https://doi.org/10.1016/j.bpsc.2022.12.005

Parmigiani, S., Zattera, B., Barchiesi, G., & Cattaneo, L. (2018). Spatial and temporal characteristics of set-related inhibitory and excitatory inputs from the dorsal premotor cortex to the ipsilateral motor cortex assessed by dual-coil transcranial magnetic stimulation. *Brain Topography*, *31*(5), 795–810. https://doi.org/10.1007/s10548-018-0635-x

R Core Team. (2019). R: A language and Environment for Statistical Computing. R Foundation for Statistical Computing. http://www.r-project.org/

Radhu, N., Garcia Dominguez, L., Farzan, F., Richter, M. A., Semeralul, M. O., Chen, R., Fitzgerald, P. B., & Daskalakis, Z. J. (2015). Evidence for inhibitory deficits in the prefrontal cortex in schizophrenia. *Brain*, *138*(2), 483–497. https://doi.org/10.1093/BRAIN/AWU360

Rossi, S., Hallett, M., Rossini, P. M., & Pascual-Leone, A. (2009). Safety, ethical considerations, and application guidelines for the use of transcranial magnetic stimulation in clinical practice and research. *Clinical Neurophysiology*, *120*(12), 2008–2039. https://doi.org/10.1016/j.clinph.2009.08.016

Rousselet, G. A., Foxe, J. J., & Bolam, J. P. (2016). A few simple steps to improve the description of group results in neuroscience. *European Journal of Neuroscience*, *44*(9), 2647–2651. https://doi.org/10.1111/ejn.13400

Saari, J., Kallioniemi, E., Tarvainen, M., & Julkunen, P. (2018). Oscillatory TMS-EEG-responses as a measure of the cortical excitability threshold. *IEEE Transactions on Neural Systems and Rehabilitation Engineering*, *26*(2), 383–391. https://doi.org/10.1109/TNSRE.2017.2779135

Sahni, V., Engmann, A., Ozkan, A., & Macklis, J. D. (2020). Motor cortex connections. In *Neural circuit and cognitive development*. Academic Press. https://doi.org/10.1016/b978-0-12-814411-4.00008-1

Sakai, K., Ugawa, Y., Terao, Y., Hanajima, R., Furubayashi, T., & Kanazawa, I. (1997). Preferential activation of different I waves by transcranial magnetic stimulation with a figure-of-eight-

shaped coil. *Experimental Brain Research*, *113*(1), 24–32. https://doi.org/10.1007/BF02454139

Siebner, H. R., Funke, K., Aberra, A. S., Antal, A., Bestmann, S., Chen, R., Classen, J., Davare, M., di Lazzaro, V., Fox, P. T., Hallett, M., Karabanov, A. N., Kesselheim, J., Beck, M. M., Koch, G., Liebetanz, D., Meunier, S., Miniussi, C., Paulus, W., … Ugawa, Y. (2022). Transcranial magnetic stimulation of the brain: What is stimulated? – A consensus and critical position paper. *Clinical Neurophysiology*, *140*, 59–97. https://doi.org/10.1016/J.CLINPH.2022.04.022

Sommer, M., Alfaro, A., Rummel, M., Speck, S., Lang, N., Tings, T., & Paulus, W. (2006). Half sine, monophasic and biphasic transcranial magnetic stimulation of the human motor cortex. *Clinical Neurophysiology*, *117*(4), 838–844. https://doi.org/10.1016/j.clinph.2005.10.029

Sommer, M., Ciocca, M., Chieffo, R., Hammond, P., Neef, A., Paulus, W., Rothwell, J. C., & Hannah, R. (2018). TMS of primary motor cortex with a biphasic pulse activates two independent sets of excitable neurones. *Brain Stimulation*, *11*(3), 558–565. https://doi.org/10.1016/j.brs.2018.01.001

Spampinato, D. (2020). Dissecting two distinct interneuronal networks in M1 with transcranial magnetic stimulation. *Experimental Brain Research*, *238*(7–8), 1693–1700. https://doi.org/10.1007/s00221-020-05875-y

Terao, Y., Ugawa, Y., Suzuki, M., Sakai, K., Hanajima, R., Gemba-Shimizu, K., & Kanazawa, I. (1997). Shortening of simple reaction time by peripheral electrical and submotor-threshold magnetic cortical stimulation. *Experimental Brain Research*, *115*(3), 541–545. https://doi.org/10.1007/PL00005724

Tervo, A. E., Nieminen, J. O., Lioumis, P., Metsomaa, J., Souza, V. H., Sinisalo, H., Stenroos, M., Sarvas, J., & Ilmoniemi, R. J. (2022). Closed-loop optimization of transcranial magnetic stimulation with electroencephalography feedback. *Brain Stimulation*, *15*, 523–531. https://doi.org/10.1016/j.brs.2022.01.016

The Jamovi Project. (2022). Jamovi (version 2.3) [Computer Software]. Retrieved from https://www.jamovi.org

Voineskos, D., Blumberger, D. M., Zomorrodi, R., Rogasch, N. C., Farzan, F., Foussias, G., Rajji, T. K., & Daskalakis, Z. J. (2019). Altered transcranial magnetic stimulation–electroencephalographic markers of inhibition and excitation in the dorsolateral prefrontal cortex in major depressive disorder. *Biological Psychiatry*, *85*(6), 477–486. https://doi.org/10.1016/J.BIOPSYCH.2018.09.032

Werhahn, K. J., Fong, J. K. Y., Meyer, B. U., Priori, A., Rothwell, J. C., Day, B. L., & Thompson, P. D. (1994). The effect of magnetic coil orientation on the latency of surface EMG and single motor unit responses in the first dorsal interosseous muscle. *Electroencephalography and Clinical Neurophysiology/Evoked Potentials Section*, *93*(2), 138–146. https://doi.org/10.1016/0168-5597(94)90077-9

Weyh, T., Wendicke, K., Mentschel, C., Zantow, H., & Siebner, H. R. (2005). Marked differences in the thermal characteristics of figure-of-eight shaped coils used for repetitive transcranial magnetic stimulation. *Clinical Neurophysiology*, *116*(6), 1477–1486. https://doi.org/10.1016/j.clinph.2005.02.002

Yuen, K. (1974). The two-sample trimmed t for unequal population variances. *Biometrika*, *61*(1), 165–170. https://doi.org/10.1093/biomet/61.1.165

Zazio, A., Barchiesi, G., Ferrari, C., Marcantoni, E., & Bortoletto, M. (2022). M1-P15 as a cortical marker for transcallosal inhibition: A preregistered TMS-EEG study. *Frontiers in Human Neuroscience*, *16*, 937515. https://doi.org/10.3389/fnhum.2022.937515

Zazio, A., Miniussi, C., & Bortoletto, M. (2021). Alpha-band cortico-cortical phase synchronization is associated with effective connectivity in the motor network. *Clinical Neurophysiology*, *132*(10), 2473–2480. https://doi.org/10.1016/J.CLINPH.2021.06.025

SUPPORTING INFORMATION

Additional supporting information can be found online in the Supporting Information section at the end of this article.

How to cite this article: Guidali, G., Zazio, A., Lucarelli, D., Marcantoni, E., Stango, A., Barchiesi, G., & Bortoletto, M. (2023). Effects of transcranial magnetic stimulation (TMS) current direction and pulse waveform on cortico-cortical connectivity: A registered report TMS-EEG study. *European Journal of Neuroscience*, 1–25. https://doi.org/10.1111/ejn.16127